



Davinder Kumar · Dilbag Singh · Sushil K. Tomar ·
Sohichi Hirose  · Takahiro Saitoh · Akira Furukawa ·
Taizo Maruyama

Reflection of plane waves from the stress-free boundary of a nonlocal elastic solid half-space containing double porosity

Received: 16 February 2022 / Accepted: 7 February 2023 / Published online: 6 March 2023
© The Author(s) 2023

Abstract Reflection phenomena of a set of coupled longitudinal waves/shear wave striking obliquely against the mechanically stress-free boundary surface of a uniform nonlocal elastic solid half-space with double porosity structure have been investigated. Employing the appropriate nonlocal stress-free boundary conditions at the surface, the formulae for reflection coefficients and their corresponding energy ratios have been derived for the dissipative and non-dissipative models. Their variations have been computed against the angle of incidence for a specific model. It is found that all the reflection coefficients depend upon the presence of the nonlocality, porosities of both types, frequency and angle of incidence. Their impact on various coefficients is also studied numerically and depicted graphically.

Keywords Double porosity · Nonlocal boundary conditions · Snell's law · Reflection · Energy

D. Kumar · D. Singh · S. K. Tomar
Department of Mathematics, Panjab University, Chandigarh 160 014, India
E-mail: davinderkgoriwal@gmail.com

S. K. Tomar
E-mail: sktomar66@gmail.com

D. Singh
University Grants Commission, New Delhi 110 002, India
E-mail: kahlondilbag80@gmail.com

S. Hirose (✉)
Department of Civil and Environmental Engineering, Tokyo Institute of Technology, Ookayama, Meguro, Tokyo 152 8550, Japan
E-mail: shirose@cv.titech.ac.jp

T. Saitoh
Department of Civil and Environmental Engineering, Gunma University, Tenjin, Kiryu, Gunma 376 8515, Japan
E-mail: t-saitoh@gunma-u.ac.jp

A. Furukawa
Division of Civil Engineering, Hokkaido University, Sapporo, Hokkaido 060 8628, Japan
E-mail: afurukawa@eng.hokudai.ac.jp

T. Maruyama
Department of Engineering for Production and Environment, Ehime University, Matsuyama, Ehime 790 8577, Japan
E-mail: maruyama@cee.ehime-u.ac.jp

1 Introduction

The problems of propagation of elastic waves and their reflection/transmission phenomena from the discontinuous boundary surfaces in elastic materials have been of continued interest since long. Elastic waves traveling through the Earth's medium are called seismic waves, and the subject dealing with the study of these waves is called seismology. Knowing the fact that the Earth is multilayered media made up of different materials possessing different characteristics, seismic waves suffer from reflection and transmission phenomena at the discontinuities between the different layers. These reflected and transmitted waves carry a lot of information about the medium through which they travel. They are also very helpful in the exploration of Earth's interior and valuable deposits beneath the earth surface like minerals, oils and hydrocarbons, etc. The reflection/transmission phenomena of elastic waves find applications in the field of geophysics, earthquake engineering, seismology, etc. The literature pertaining to the reflection and transmission phenomena of elastic waves from the boundary surfaces in classical elastic media is available in abundance, for example, see Ewing et al. [1], Achenbach [2], Aki and Richards [3], among several others. Around 1980s, the classical elastic theory was extended to the theory of elastic materials with voids by Cowin and his co-worker [4,5]. An elastic material with voids is a porous material, whose skeletal or matrix material is elastic and the voids are vacuum pores containing nothing of mechanical or energetic significance, but occupy certain surface area and volume. The bulk density of the material is written as a product of the density of the matrix material and the void volume fractional field. In this theory, the deformation involves the strain field related to matrix material along with the change in void volume fractional field associated with the voids of the medium. The change in void volume fraction is introduced as an independent additional kinematic variable along with an associated force termed as "equilibrated stress." Incorporating void volume fraction and the associated force, the constitutive relations and field equations for homogeneous isotropic elastic material with voids were developed. Using this theory, Puri and Cowin [6] explored the possibility of plane wave propagation in an infinite elastic material with voids and found that there may exist three plane waves propagating with distinct speeds. Two of them are coupled dilatational waves influenced by the presence of voids, while the remaining one is an independent transverse wave, which is no different from the classical shear wave. Ciarletta and Sumbatyan [7] investigated the reflection phenomena of incident coupled longitudinal waves/shear wave from the stress-free boundary of an elastic half-space with voids. Ieşan [8] extended the theory of elastic material with voids to thermoelastic material with voids by incorporating the theory of coupled thermoelasticity. Later, Ieşan and Quintanilla [9] developed the nonlinear and linear theories of thermoelastic materials possessing double porosity structure and presented the field equations for homogeneous isotropic material. Using their theory, Svanadze [10,11] studied the plane harmonic waves and uniqueness theorems in the theory of rigid/elastic bodies with double porosity structure. He presented the connection between the plane waves, uniqueness of solutions and existence of eigenfrequencies. Singh et al. [12] explored the propagation of plane harmonic waves in an infinite thermoelastic medium with double porosity structure and also studied the reflection of coupled longitudinal waves from the insulated and stress-free boundary surface. Some recent research articles dealing with the theory of elastic solid with single/double voids are attempted by Biswas and Abo-Dahab [13], Long and Fan [14], Kumar and Tomar [15] and De Cicco [16]. The detailed literature about double/multi-porosity continua and its mathematical aspects have been nicely presented in a book by Straughan [17].

In the nonlocal theory of elasticity, introduced by Eringen and his co-worker (see Eringen and Edelen [18] and Eringen [19,20]), the stresses at a point in the region of a continuum body depend not only on the strains at that point but also on the strains at all its surrounding points by considering the remote action forces between the atoms unlike classical elasticity. It is emphasized that the nonlocal effect becomes more prominent when the external characteristic length (e.g., wavelength, size of the sample) and the internal characteristic length (e.g., the lattice parameter, size of the grain) are comparable while dealing with the problems of waves and vibrations. In nano-materials such as carbon nanotubes, the length scales are sufficiently small and it is found that Eringen's nonlocal model is most suitable for dealing with such models. Some notable researches based on Eringen's nonlocal theory of elasticity are contained in Altan [21,22], Chirita [23], Shaat et al. [24], among several others. Using Eringen's model of nonlocality, Singh et al. [25] developed the theory of nonlocal elastic materials with voids and derived the field equations. They have also investigated the propagation of plane waves and their reflection from the stress-free boundary surface by using local boundary conditions. They found that all the reflection coefficients are influenced by the presence of nonlocality and presence of voids in the medium. They observed that the reflection coefficients corresponding to the coupled longitudinal waves increase, while the reflection coefficients corresponding to the transverse wave decrease with an increase in the nonlocality parameter of the medium when a set of coupled longitudinal waves is made incident. Several authors [26]–[31]

have attempted reflection/transmission of plane waves in nonlocal media to study the effect of nonlocality on reflection/transmission coefficients by using appropriate local boundary conditions. Recently, Kumar et al. [32] developed the theory of nonlocal elastic material with double porosity structure by incorporating additional voids in the theory of nonlocal elastic solid with voids [25]. They have explored the propagation of plane harmonic waves in an infinite nonlocal elastic materials with double porosity structure.

In the present work, we investigated the reflection phenomenon of plane waves from the stress-free boundary surface of a nonlocal elastic half-space having double porosity structure using nonlocal boundary conditions. The reflection coefficients and the corresponding energy ratios are derived when a set of plane coupled longitudinal waves/transverse wave is made incident obliquely at the stress-free surface of the half-space. All the reflection coefficients and corresponding energy ratios are found to be the functions of nonlocality, porosity, elastic properties, frequency and angle of incidence. For a particular numerical model, the effect of various parameters corresponding to voids and nonlocality is studied numerically on the reflection coefficients and depicted graphically. Some reduced cases have been analyzed from the present formulation.

2 Relations and equations

Following Kumar et al. [32], the constitutive relations for nonlocal elastic solid containing double porosity within the context of Eringen's nonlocal model of elasticity are given by

$$(1 - \epsilon^2 \nabla^2) t_{ij} = t_{ij}^L = 2\mu e_{ij}(\mathbf{x}) + (\lambda e_{kk}(\mathbf{x}) + b\phi(\mathbf{x}) + d\psi(\mathbf{x}))\delta_{ij}, \quad (1)$$

$$(1 - \epsilon^2 \nabla^2) \xi = \xi^L = -\tau_\phi \dot{\phi}(\mathbf{x}) - \alpha_1 \phi(\mathbf{x}) - b e_{ii}(\mathbf{x}) - \alpha_3 \psi(\mathbf{x}), \quad (2)$$

$$(1 - \epsilon^2 \nabla^2) \sigma_i^{(1)} = (\sigma_i^{(1)})^L = \alpha \phi_{,i}(\mathbf{x}) + b_1 \psi_{,i}(\mathbf{x}), \quad (3)$$

$$(1 - \epsilon^2 \nabla^2) \zeta = \zeta^L = -\tau_\psi \dot{\psi}(\mathbf{x}) - \alpha_3 \phi(\mathbf{x}) - d e_{ii}(\mathbf{x}) - \alpha_2 \psi(\mathbf{x}), \quad (4)$$

$$(1 - \epsilon^2 \nabla^2) \sigma_i^{(2)} = (\sigma_i^{(2)})^L = b_1 \phi_{,i}(\mathbf{x}) + \gamma \psi_{,i}(\mathbf{x}), \quad (5)$$

where $i, j = 1, 2, 3$; ∇^2 is the Laplacian operator; ϵ is the nonlocality parameter defined by $\epsilon = e_0 a$, e_0 is the material constant and a is the internal characteristic length depending upon the material properties. The local constitutive parameters λ and μ are Lamé constants. t_{ij} is the nonlocal stress tensor, τ_ϕ and τ_ψ are the dissipation parameters; $\sigma_i^{(1)}$ and $\sigma_i^{(2)}$ are the nonlocal equilibrated stress vectors; ξ and ζ are the nonlocal intrinsic equilibrated body forces; ϕ and ψ are the change in void volume fractions corresponding to the first and second kind of voids, respectively; e_{ij} is the Lagrangian strain tensor in the context of linear theory; δ_{ij} is the Kronecker delta. The constitutive coefficients $b, d, \alpha_1, \alpha_2, \alpha_3, \alpha, \gamma$ and b_1 are the void parameters corresponding to the first and second type of voids. A superscripted dot represents the partial time derivative. The superscript "L" represents the local effects and \mathbf{x} is the local point in the considered material. An index followed by a comma indicates partial differentiation with respect to spatial variable.

The equations of motion for the linear isotropic nonlocal elastic materials with double porosity structure in the absence of body forces and after applying the Helmholtz decomposition on displacement vector \mathbf{u} by introducing scalar and vector potential p and \mathbf{U} , respectively, are given by (see Kumar et al. [32])

$$(\lambda + 2\mu)\nabla^2 p + b\phi + d\psi = \rho(1 - \epsilon^2 \nabla^2) \ddot{p}, \quad (6)$$

$$\nabla^2(\alpha\phi + b_1\psi - bp) - (\alpha_1\phi + \alpha_3\psi + \tau_\phi \dot{\phi}) = (1 - \epsilon^2 \nabla^2) \chi_1 \ddot{\phi}, \quad (7)$$

$$\nabla^2(b_1\phi + \gamma\psi - dp) - (\alpha_3\phi + \alpha_2\psi + \tau_\psi \dot{\psi}) = (1 - \epsilon^2 \nabla^2) \chi_2 \ddot{\psi}, \quad (8)$$

$$\mu \nabla^2 \mathbf{U} = \rho(1 - \epsilon^2 \nabla^2) \dot{\mathbf{U}}. \quad (9)$$

Here, ρ is the mass density; χ_1 and χ_2 , respectively, represent the equilibrated inertia per unit mass per unit volume corresponding to the first and second kind of voids. Note that the equations (6)-(8) are coupled in scalar potentials p, ϕ and ψ , while equation (9) is independent in vector potential \mathbf{U} .

3 Wave propagation

Kumar et al. [32] have explored the possibility of propagation of plane harmonic waves in an infinite nonlocal elastic material possessing double porosity. They found that there may propagate three sets of coupled longitudinal waves and a lone shear wave traveling at distinct speeds. Each set of coupled longitudinal waves is

influenced by the presence of nonlocality and voids in the medium, while the lone shear wave is affected by the presence of nonlocality only. Borrowing the notations of Kumar et al. [32], the speeds of traveling waves and coupling parameters are given as follows.

(a) The speeds of three coupled longitudinal waves are given by the roots of the following bicubic equation:

$$Pc^6 + Qc^4 + Rc^2 + S = 0, \tag{10}$$

where the expression of coefficients P , Q , R and S is given as

$$\begin{aligned} P &= \rho[\eta_0 + \omega(\iota\chi_0 - \tau_\phi\tau_\psi\omega)], \\ Q &= -(\mu_0\eta_0 + \varsigma_1) + \omega^2(\tau_\phi\tau_\psi\mu_0 - \rho\varsigma_0) - \iota\omega(b^2\tau_\psi + d^2\tau_\phi + \mu_0\chi_0) \\ &\quad - \rho\omega^3[\Upsilon_1 - \epsilon^2(2\omega^2\Upsilon_3 - \alpha_1\tau_\psi - \alpha_2\tau_\phi)] \\ &\quad + \rho\epsilon^2\omega^2[\beta_0 + 3\chi_1\chi_2\omega^4 - 2\omega^2\Upsilon_2 - \tau_\phi\tau_\psi\epsilon^2], \\ R &= \omega^2[\mu_0\varsigma_0 + \beta_1 + \rho\alpha_0\omega^2 - \epsilon^2(\chi_2b^2 + \chi_1d^2) \\ &\quad + \iota\omega(\mu_0 - \rho\epsilon^2\omega^2)[\Upsilon_1 - \epsilon^2\omega(\iota\Upsilon_2 + \omega\Upsilon_3)] \\ &\quad - 2\rho\epsilon^2\omega^4(\chi_2\alpha_1 + \chi_1\gamma) + \rho\epsilon^2\omega^2(\alpha\alpha_2 + \gamma\alpha_1 - 2\alpha_3b_1) \\ &\quad - \chi_1\chi_2\epsilon^2\omega^4(2\mu_0 - 3\rho\epsilon^2\omega^2)], \\ S &= \omega^4[\chi_1\chi_2\epsilon^4\omega^4 - (\chi_2\alpha + \chi_1\gamma)\epsilon^2\omega^2 + \alpha_0](\rho\epsilon^2\omega^2 - \mu_0), \\ \eta_1 &= \chi_1\omega^2 - \alpha_1, \quad \eta_2 = \chi_2\omega^2 - \alpha_2, \quad \mu_0 = \lambda + 2\mu, \quad \alpha_0 = \alpha\gamma - b_1^2, \\ \varsigma_0 &= \alpha\eta_2 + \gamma\eta_1 + 2b_1\alpha_3, \quad \varsigma_1 = d^2\eta_1 + b^2\eta_2 + 2bd\alpha_3, \quad \beta_0 = \alpha_1\alpha_2 - \alpha_3^2, \\ \chi_0 &= \eta_1\tau_\psi + \eta_2\tau_\phi, \quad \eta_0 = \eta_1\eta_2 - \alpha_3^2, \quad \beta_1 = \alpha d^2 + \gamma b^2 - 2bdb_1, \\ \Upsilon_1 &= \alpha\tau_\psi + \gamma\tau_\phi, \quad \Upsilon_2 = \chi_1\alpha_2 + \chi_2\alpha_1, \quad \Upsilon_3 = \chi_1\tau_\psi + \chi_2\tau_\phi. \end{aligned}$$

Here, ω denotes the angular frequency, which is related to the speed c and wavenumber k through relation $\omega = kc$. Since the coefficients of bicubic equation (10) are complex-valued, there exist six complex-valued roots. Among these six roots, three will have positive real part representing the speeds of three sets of coupled longitudinal waves advancing in positive direction. We shall denote these roots by c_1 , c_2 and c_3 representing the speeds of three sets of coupled longitudinal waves.

(b) The speed of lone shear wave is given by $c_4 = \sqrt{c_t^2 - \epsilon^2\omega^2}$; c_t being the speed of the shear wave in classical elastic medium.

The phase speeds V_i , ($i = 1, 2, 3, 4$) and their corresponding attenuation coefficients Q_i , ($i = 1, 2, 3, 4$) of these waves propagating in the medium can be obtained from the formulae given by Borchardt [33], which are as follows:

$$V_i = \frac{[\Re(c_i)]^2 + [\Im(c_i)]^2}{\Re(c_i)}, \quad Q_i = -\frac{\omega\Im(c_i)}{[\Re(c_i)]^2 + [\Im(c_i)]^2}.$$

Here, $\Re(\cdot)$ and $\Im(\cdot)$ represent, respectively, the real and imaginary parts of (\cdot) .

The expressions of coupling parameters Ω_{2c} and Ω_{3c} between the displacement and change in void volume fraction of the first and second type of voids, respectively, are given by

$$\begin{aligned} \Omega_{2c} &= \frac{\rho\omega^2(c_\ell^2 - \epsilon^2\omega^2 - c^2) + d\Omega_{3c}c^2}{bc^2}, \\ \Omega_{3c} &= \frac{(d + Ab)\omega^2}{\omega^2(Ab_1 - \epsilon^2\omega^2\chi_2 + \gamma) + c^2(A\alpha_3 - \iota\omega\tau_\psi - \eta_2)}, \end{aligned}$$

and

$$A = \frac{b_1\omega^2 + \alpha_3c^2}{\omega^2(\epsilon^2\omega^2\chi_1 - \alpha) + c^2(\eta_1 + \iota\omega\tau_\phi)}, \quad c_\ell^2 = \frac{\lambda + 2\mu}{\rho}.$$

The detailed discussion about these coupling parameters can be seen in Kumar et al. [32].

4 Reflection phenomenon

We considered an isotropic and homogeneous nonlocal elastic solid half-space possessing double porosity structure. With reference to a rectangular Cartesian coordinate system $Oxyz$, the considered half-space can be defined as

$$M = \{(x, y, z); -\infty < x, y < \infty, 0 \leq z < \infty\},$$

whose boundary surface is given by $z = 0$ and z -axis is pointing vertically downward into the half-space. For a two-dimensional problem in $x - z$ plane, the displacement components and change in void volume fractions can be taken as

$$\mathbf{u}(x, z, t) = (u(x, z, t), 0, w(x, z, t)), \quad \phi = \phi(x, z, t), \quad \psi = \psi(x, z, t),$$

along with $\partial(\cdot)/\partial y = 0$. As explained earlier in Sect. 2, the relevant components of displacement vector \mathbf{u} are given by

$$u = p_{,x} - U_{,z}, \quad w = p_{,z} + U_{,x}, \quad (11)$$

where U is the y -component of vector \mathbf{U} .

We consider a set of coupled longitudinal waves/shear wave traveling through half-space M with phase speed V_n , ($n = 1, 2, 3, 4$), having amplitude A_{0n} and striking obliquely at the boundary $z = 0$ of the half-space M making an angle θ_n with the normal to the boundary surface. We shall assume that the boundary surface $z = 0$ of the half-space M is mechanically stress-free. In order to satisfy the boundary conditions at the free surface, we postulate the existence of following reflected waves as:

1. Three sets of coupled longitudinal waves with amplitudes A_i , ($i = 1, 2, 3$), traveling with phase speeds V_i and making angles θ_i , respectively, with the normal.
2. An independent shear wave with amplitude A_4 traveling with phase speed V_4 and making an angle θ_4 with the normal.

The total wave field in the considered half-space M can be written as

(i) For the incidence of a set of time harmonic plane coupled longitudinal waves propagating with phase speed V_n , ($n = 1, 2, 3$), we have

$$\begin{aligned} \{p, \phi, \psi\} &= A_{0n} \{1, \Omega_{2c_n}, \Omega_{3c_n}\} \exp\{tk_n(x \sin \theta_n - z \cos \theta_n) - \iota\omega t\} \\ &+ \sum_{i=1}^3 A_i \{1, \Omega_{2c_i}, \Omega_{3c_i}\} \exp\{tk_i(x \sin \theta_i + z \cos \theta_i) - \iota\omega t\}, \end{aligned} \quad (12)$$

$$U = A_4 \exp\{tk_4(x \sin \theta_4 + z \cos \theta_4) - \iota\omega t\}. \quad (13)$$

(ii) For the incidence of a plane shear wave propagating with phase speed V_4 , we have

$$\{p, \phi, \psi\} = \sum_{i=1}^3 A_i \{1, \Omega_{2c_i}, \Omega_{3c_i}\} \exp\{tk_i(x \sin \theta_i + z \cos \theta_i) - \iota\omega t\}, \quad (14)$$

$$\begin{aligned} U &= A_{04} \exp\{tk_4(x \sin \theta_4 - z \cos \theta_4) - \iota\omega t\} \\ &+ A_4 \exp\{tk_4(x \sin \theta_4 + z \cos \theta_4) - \iota\omega t\}, \end{aligned} \quad (15)$$

where ω is the common angular frequency, k_i is the wavenumber, which is related to the phase speed V_i through the relation $k_i = \omega/V_i$, ($i = 1, 2, 3, 4$). The expressions of coupling parameters $\Omega_{2c_i}, \Omega_{3c_i}$, ($i = 1, 2, 3$) can be obtained from the expression of Ω_{2c}, Ω_{3c} by replacing c with c_i . The stress-free boundary conditions must be satisfied for any x and t on the boundary surface $z = 0$, and all exponentials in (12)–(15) must be common. Therefore, we have the Snell's law given by

$$\frac{\sin \theta_n}{V_n} = \frac{\sin \theta_i}{V_i} = k_0/\omega, \quad i = 1, 2, 3, 4. \quad (16)$$

Here, k_0 is an apparent wavenumber.

4.1 Nonlocal boundary conditions and reflection coefficients

The boundary surface of the half-space M is assumed to be mechanically stress-free; therefore, all nonlocal stresses must vanish at the surface, i.e., $t_{zz} = t_{zx} = \sigma_z^{(1)} = \sigma_z^{(2)} = 0$ at $z = 0$. The nonlocal stresses can be obtained in terms of local stresses by operating $(1 - \epsilon^2 \nabla^2)^{-1}$ to both sides of (1)-(5) (See Eringen [34]). We shall assume that the nonlocal parameter ϵ is so small that its third and higher powers are negligible. Thus, by using (11) the nonlocal boundary conditions can now be written in terms of the potentials p, ϕ, ψ and U as

$$(1 + \epsilon^2 \nabla^2) [(\lambda + 2\mu)\nabla^2 p + 2\mu(U_{,zx} - p_{,xx}) + (b\phi + d\psi)] = 0, \tag{17}$$

$$(1 + \epsilon^2 \nabla^2) (2p_{,xz} - U_{,zz} + U_{,xx}) = 0, \tag{18}$$

$$(1 + \epsilon^2 \nabla^2) (\alpha\phi_{,z} + b_1\psi_{,z}) = 0, \tag{19}$$

$$(1 + \epsilon^2 \nabla^2) (b_1\phi_{,z} + \gamma\psi_{,z}) = 0. \tag{20}$$

Here, the approximation $(1 - \epsilon^2 \nabla^2)^{-1} \approx (1 + \epsilon^2 \nabla^2)$ has been used as the higher-order terms are negligible. Inserting the expressions of potentials given in (12)-(15) into the boundary conditions (17)-(20), we obtain a system of four non-homogeneous linear equations in four unknowns. This system of equations can be written in matrix form as

$$[a_{ij}][X_j] = [b_i], \tag{21}$$

where $[a_{ij}]$ is a 4×4 square matrix, $[X_j]$ and $[b_i]$ are 4×1 column vectors. The nonzero entries of matrix $[a_{ij}]$ are given by

$$\begin{aligned} a_{1j} &= R_j K_j, \quad a_{14} = 2\mu K_4 \cot \theta_4, \quad a_{2j} = 2K_j \cot \theta_j, \quad a_{24} = K_4(1 - \cot^2 \theta_4), \\ a_{3j} &= G_j K_j \cot \theta_j, \quad a_{4j} = H_j K_j \cot \theta_j, \\ G_j &= \alpha \Omega_{2c_j} + b_1 \Omega_{3c_j}, \quad H_j = b_1 \Omega_{2c_j} + \gamma \Omega_{3c_j}, \\ R_j &= \left[\lambda + (\lambda + 2\mu) \cot^2 \theta_j - \frac{b}{k_0^2} \Omega_{2c_j} - \frac{d}{k_0^2} \Omega_{3c_j} \right], \quad j = 1, 2, 3, \\ K_m &= 1 - \epsilon^2 k_0^2 (1 + \cot^2 \theta_m), \quad m = 1, 2, 3, 4. \end{aligned} \tag{22}$$

The entries of column vector $[b_i]$ are given by

(i) For the incidence of coupled longitudinal waves having phase speed V_n , ($n = 1, 2, 3$), we have

$$b_1 = -R_n K_n, \quad b_2 = 2K_n \cot \theta_n, \quad b_3 = G_n K_n \cot \theta_n, \quad b_4 = H_n K_n \cot \theta_n. \tag{23}$$

(ii) For the incidence of shear wave having phase speed V_4 , we have

$$b_1 = 2\mu K_4 \cot \theta_4, \quad b_2 = K_4(\cot^2 \theta_4 - 1), \quad b_3 = b_4 = 0. \tag{24}$$

The entries $X_i (= \frac{A_i}{A_{0n}})$, $i = 1, 2, 3, 4$ represent the reflection coefficients corresponding to the four reflected waves.

On solving the matrix equation (21), the expressions of various reflection coefficients are obtained in closed form as

(i) For the incidence of coupled longitudinal waves having phase speed V_n , ($n = 1, 2, 3$), we obtain

$$\begin{aligned} X_1 &= \frac{K_n \left\{ 4\mu \cot \theta_2 \cot \theta_3 \cot \theta_4 \cot \theta_n \tilde{M}_n - (\cot^2 \theta_4 - 1) \tilde{\Gamma}_n \right\}}{K_1 \left\{ 4\mu \cot \theta_1 \cot \theta_2 \cot \theta_3 \cot \theta_4 M_1 + (\cot^2 \theta_4 - 1) \Gamma_1 \right\}}, \\ X_2 &= \frac{L_{n3} K_n \cot \theta_n - L_{13} K_1 \cot \theta_1 X_1}{L_{23} K_2 \cot \theta_2}, \\ X_3 &= \frac{(H_n L_{23} - H_2 L_{n3}) K_n \cot \theta_n - (H_1 L_{23} - H_2 L_{13}) K_1 \cot \theta_1 X_1}{H_3 K_3 L_{23}^2 \cot \theta_3}, \end{aligned}$$

$$X_4 = - \frac{K_n \tilde{\Gamma}_n + K_1 \Gamma_1 X_1}{2\mu \cot \theta_2 \cot \theta_3 \cot \theta_4 K_4 H_3 L_{23}}$$

(ii) For the incidence of shear wave having phase speed V_4 , we obtain

$$\begin{aligned} X_1 &= \frac{4\mu \cot \theta_2 \cot \theta_3 \cot \theta_4 (\cot^2 \theta_4 - 1) K_4 G_3 L_{32}}{K_1 \{ (G_3 F_1 \cot \theta_3 - G_1 F_3 \cot \theta_1) L_{32} \cot \theta_2 + (G_3 F_2 \cot \theta_3 - G_2 F_3 \cot \theta_2) L_{13} \cot \theta_1 \}}, \\ X_2 &= \frac{K_1 L_{13} \cot \theta_1 X_1}{K_2 L_{32} \cot \theta_2}, \quad X_3 = \frac{K_1 (G_1 L_{23} + G_2 L_{31}) \cot \theta_1 X_1}{K_3 G_3 L_{32} \cot \theta_3}, \\ X_4 &= -1 + \frac{2K_1 \cot \theta_1 X_1}{K_4 (\cot^2 \theta_4 - 1)} \left[1 + \frac{L_{13}}{L_{32}} + \frac{G_1 L_{23} + G_2 L_{31}}{G_3 L_{32}} \right]. \end{aligned}$$

The expressions of various symbols used above are as follows:

$$\begin{aligned} L_i &= H_3 - H_i, \quad \tilde{L}_n = H_3 - H_n, \quad L_{ij} = G_i H_j - G_j H_i, \quad i, j = 1, 2, 3 \\ M_1 &= L_1 L_{23} - L_2 L_{13}, \quad \tilde{M}_n = \tilde{L}_n L_{23} - L_2 L_{n3}, \quad N_i = H_3 R_i \cot \theta_3 - H_i R_3 \cot \theta_i, \\ \Gamma_1 &= N_1 L_{23} \cot \theta_2 - N_2 L_{13} \cot \theta_1, \quad \tilde{N}_n = H_3 R_n \cot \theta_3 + H_n R_3 \cot \theta_n, \\ \tilde{\Gamma}_n &= \tilde{N}_n L_{23} \cot \theta_2 + N_2 L_{n3} \cot \theta_n, \quad F_n = R_n (\cot^2 \theta_4 - 1) + 4\mu \cot \theta_4 \cot \theta_n. \end{aligned}$$

We note that the reflection coefficients under both the cases (i) and (ii) depend upon nonlocality parameter, voids parameters, angle of incidence, frequency and the material properties. All the reflection coefficients are found to be complex-valued due to the presence of dissipation parameters τ_ϕ and τ_ψ in their expressions. For non-dissipative model, the reflection coefficients can be easily obtained by setting $\tau_\phi = \tau_\psi = 0$ in the above expressions.

5 Special cases

5.1 Nonlocal elastic solid with single porosity

In the absence of one kind of voids from the medium, we shall be left with the nonlocal elastic solid with single type of voids. For definiteness, setting the parameters corresponding to the second type of voids to zero, i.e., $d = \gamma = b_1 = \alpha_2 = \alpha_3 = \chi_2 = 0$, we see that $V_2 = \Omega_{3c} = A_2 = 0$ and equation (20) is satisfied identically. Then, the matrix equation (21) reduces to a system of three non-homogeneous equations given by

$$[a'_{ij}][X'_j] = [b'_i], \quad i, j = 1, 3, 4.$$

The nonzero entries of matrix $[a'_{ij}]$ are given as

$$\begin{aligned} a'_{1j} &= R'_j K_j, \quad a'_{14} = 2\mu K_4 \cot \theta_4, \quad a'_{2j} = 2K_j \cot \theta_j, \\ a'_{24} &= K_4 (1 - \cot^2 \theta_4), \quad a'_{3j} = \Omega'_{2c_j} K_j \cot \theta_j, \end{aligned}$$

where

$$R'_j = \lambda + (\lambda + 2\mu) \cot^2 \theta_j - \frac{b}{k_0^2} \Omega'_{2c_j}, \quad \Omega'_{2c_j} = \frac{\rho \omega^2}{bc_j^2} \left[c_\ell^2 - (c_j^2 + \epsilon^2 \omega^2) \right], \quad j = 1, 3.$$

The entries of column vector $[b'_i]$ are given by

(i) For the incidence of coupled longitudinal waves having phase speed V_n , ($n = 1, 3$), we have

$$b'_1 = -R'_n K_n, \quad b'_3 = 2K_n \cot \theta_n, \quad b'_4 = K_n \cot \theta_n, \quad n = 1, 3.$$

(ii) For the incidence of shear wave having phase speed V_4 , we have

$$b'_1 = 2\mu K_4 \cot \theta_4, \quad b'_3 = K_4 (\cot^2 \theta_4 - 1), \quad b'_4 = 0.$$

The reflection coefficients for case (i) are obtained as

$$X'_1 = \frac{K_n \{4\mu B_n \cot \theta_3 \cot \theta_4 \cot \theta_n - \tilde{N}_n(\cot^2 \theta_4 - 1)\}}{K_1 \{4\mu B_1 \cot \theta_1 \cot \theta_3 \cot \theta_4 + N'_1(\cot^2 \theta_4 - 1)\}},$$

$$X'_3 = \frac{\Omega'_{2c_n} K_n \cot \theta_n - \Omega'_{2c_1} K_1 \cot \theta_1 X'_1}{\Omega'_{2c_3} K_3 \cot \theta_3}, \quad X'_4 = 2 \frac{\cot \theta_1 K_1 B_1 X'_1 - \cot \theta_n B_n K_n}{\Omega'_{2c_3} K_4 (\cot^2 \theta_4 - 1)}.$$

The reflection coefficients for case (ii) are obtained as

$$X'_1 = \frac{4\mu K_4 \Omega'_{2c_3} \cot \theta_3 \cot \theta_4 (\cot^2 \theta_4 - 1)}{K_1 \{N'_1(\cot^2 \theta_4 - 1) + 4\mu B_1 \cot \theta_1 \cot \theta_3 \cot \theta_4\}},$$

$$X'_3 = -\frac{\Omega'_{2c_1} K_1 \cot \theta_1 X'_1}{\Omega'_{2c_3} K_3 \cot \theta_3}, \quad X'_4 = \frac{2B_1 K_1 \cot \theta_1 X'_1 - \Omega'_{2c_3} K_4 (\cot^2 \theta_4 - 1)}{\Omega'_{2c_3} K_4 (\cot^2 \theta_4 - 1)}.$$

The expressions of various symbols used in these coefficients are given as

$$\tilde{N}_n = R'_n \Omega'_{2c_3} \cot \theta_3 + R'_3 \Omega'_{2c_n} \cot \theta_n, \quad B_n = \Omega'_{2c_3} - \Omega'_{2c_n},$$

$$N'_1 = R'_1 \Omega'_{2c_3} \cot \theta_3 - R'_3 \Omega'_{2c_1} \cot \theta_1.$$

We see that all these reflection coefficients depend upon nonlocality, void parameters and angle of incidence.

5.2 Local elastic solid with double porosity

To neglect the effect of nonlocality from the half-space, we shall set $\epsilon = 0$. Then, we shall be left with the local elastic solid with double porosity structure. In this case, each value of K_m , ($m = 1, 2, 3, 4$) becomes unity and rest the expressions of reflection coefficients remain the same as given in Subsection 5.1. The phase speeds of all the waves become independent of nonlocal parameter. Also, the coupling parameters reduce to

$$\Omega_{2c} = \frac{\rho\omega^2 c_\ell^2 - c^2(\rho\omega^2 + d\Omega_{3c})}{bc^2}, \quad \Omega_{3c} = \frac{(d + Ab)\omega^2}{\omega^2(Ab_1 + \gamma) + c^2(A\alpha_3 - i\omega\tau_\psi - \eta_2)},$$

where

$$A = \frac{b_1\omega^2 + \alpha_3 c^2}{c^2(\eta_1 + i\omega\tau_\phi) - \omega^2\alpha}.$$

We see that all the reflection coefficients become independent of nonlocality parameter.

5.3 Local elastic solid with single porosity

On setting the nonlocality parameter to zero, i.e., $\epsilon = 0$ in the model under Subsection 5.1, we shall be left with local elastic solid with voids. In this case too, each value of K_m , ($m = 1, 3, 4$) becomes unity. The expressions of all the reflection coefficients remain the same as in the Subsection 5.1 for the incidence of coupled waves or shear wave. But the phase speeds of propagating waves become independent of nonlocality and the coupling parameter reduces to

$$\Omega'_{2c} = \frac{\rho\omega^2(c_\ell^2 - c^2)}{bc^2}.$$

The expressions of all the reflection coefficients obtained under this case match with those of Ciarletta and Sumbatyan [7] for the corresponding problem apart from notations.

5.4 Nonlocal elastic solid

In the absence of void parameters from the model under Subsection 5.1, we shall be left with the nonlocal elastic solid. Setting the void parameters, i.e., α , b , α_1 and τ_ϕ to zero, we found that the phase speed of one of the coupled longitudinal waves and the corresponding amplitude and the coupling parameter vanish, i.e., $V_1 = A_1 = 0$ (say) and $\Omega'_{2c} = 0$. The expressions of reflection coefficients are obtained as

(i) For the incidence of longitudinal wave having phase speed V_3 , we obtain

$$X_3'' = \frac{-2\mu K_4 \cot \theta_4 X_4''}{K_3 [\lambda + (\lambda + 2\mu) \cot^2 \theta_3]} - 1,$$

$$X_4'' = \frac{4 \cot \theta_3 K_3 [\lambda + (\lambda + 2\mu) \cot^2 \theta_3]}{K_4 \{(1 - \cot^2 \theta_4) [\lambda + (\lambda + 2\mu) \cot^2 \theta_3] - 4\mu \cot \theta_3 \cot \theta_4\}}$$

(ii) For the incidence of shear wave having phase speed V_4 , we obtain

$$X_3'' = \frac{2\mu K_4 \cot \theta_4 (1 - \cot^2 \theta_4)}{K_3 \{(1 - \cot^2 \theta_4) [\lambda + (\lambda + 2\mu) \cot^2 \theta_4] - 4\mu \cot \theta_4\}},$$

$$X_4'' = \frac{-2K_3 \cot \theta_3 X_3''}{K_4 (1 - \cot^2 \theta_4)} - 1.$$

Here, the quantities V_3 and V_4 are the phase speed of longitudinal and shear waves, respectively, in nonlocal elastic medium.

5.5 Classical elastic solid

Further, neglecting the nonlocality from the model under Subsection 5.4, we shall be left with Cauchy elastic solid. The expressions of reflection coefficients shall remain the same as given in Subsection 5.4, and the speeds of longitudinal and shear waves will match with those of in the classical elasticity.

6 Energy partitioning

Here, we wish to find the amount of energy carried along different reflected waves out of the amount of energy carried along the incident wave. For a particular model, we shall verify that the sum of energy ratios corresponding to the various reflected waves at the boundary surface is close to unity at each angle of incidence. Following Achenbach [2], the energy flux P^* across a surface element of the boundary surface, the rate at which the energy is communicated per unit area of the surface of nonlocal elastic solid with double voids, is given by

$$P^* = t_{zz}\dot{w} + t_{zx}\dot{u} + \sigma_z^{(1)}\dot{\phi} + \sigma_z^{(2)}\dot{\psi}. \tag{25}$$

The time averaging of P^* over a complete period is denoted by $\langle P^* \rangle$, which gives the average energy transmission per unit surface area per unit time. Let $\langle P_{0n}^* \rangle$ be the time average energy carried along incident wave with phase speed V_n , ($n = 1, 2, 3, 4$) and $\langle P_i^* \rangle$, ($i = 1, 2, 3, 4$) be the time average energy carried along the reflected waves propagating with phase speeds V_i . We define the energy ratio E_i , ($i = 1, 2, 3, 4$) corresponding to the energy carried along i^{th} reflected wave at $z = 0$ to the energy carried along the incident wave as

$$E_i = \frac{\langle P_i^* \rangle}{\langle P_{0n}^* \rangle}. \tag{26}$$

The expressions of energy ratios for various reflected waves are written in closed form as

$$E_i = -X_i^2 [(\lambda + 2\mu)k_i^2 - \Omega_{2c_i}(b + \alpha\Omega_{2c_i} + b_1\Omega_{3c_i}) - \Omega_{3c_i}(d + \gamma\Omega_{3c_i} + b_1\Omega_{2c_i})]$$

$$\times K_i k_i \cos \theta_i E_0^{-1}, \tag{27}$$

$$E_4 = -X_4^2 \mu k_4^3 K_4 \cos \theta_4 E_0^{-1}, \quad i = 1, 2, 3,$$

where E_0 is the expression of energy carried along the incident wave.

The expression of E_0 is given by

(i) For the incidence of coupled longitudinal waves having speed V_n , ($n = 1, 2, 3$), we have

$$E_0 = [(\lambda + 2\mu)k_n^2 - \Omega_{2c_n}(b + \alpha\Omega_{2c_n} + b_1\Omega_{3c_n}) - \Omega_{3c_n}(d + \gamma\Omega_{3c_n} + b_1\Omega_{2c_n})] K_n k_n \cos \theta_n.$$

(ii) For the incidence of shear wave having phase speed V_4 , we have

$$E_0 = \mu K_4 k_4^3 \cos \theta_4.$$

7 Surface Response

Using equations (11)–(15), the response of the solid particles at the surface $z = 0$ of the half-space M due to the incidence of coupled longitudinal waves/shear wave propagating with phase speed V_n ($n = 1, 2, 3, 4$) can be expressed in terms of reflection coefficients. The displacement components u , w , and change in void volume fractions ϕ , ψ corresponding to the void of the first and second type, respectively, at $z = 0$ are given as follows

(i) For the incidence of coupled longitudinal waves having phase speed V_n ($n = 1, 2, 3$), we have

$$\begin{aligned} u &= \iota A_{0n} \left[k_n \sin \theta_n + \sum_{i=1}^3 k_i \sin \theta_i \left(\frac{A_i}{A_{0n}} \right) - k_4 \cos \theta_4 \left(\frac{A_4}{A_{0n}} \right) \right] \\ &\quad \times \exp\{\iota k_n x \sin \theta_n - \iota \omega t\}, \\ w &= \iota A_{0n} \left[-k_n \cos \theta_n + \sum_{i=1}^3 k_i \cos \theta_i \left(\frac{A_i}{A_{0n}} \right) - k_4 \sin \theta_4 \left(\frac{A_4}{A_{0n}} \right) \right] \\ &\quad \times \exp\{\iota k_n x \sin \theta_n - \iota \omega t\}, \\ \phi &= A_{0n} \left[\Omega_{2c_n} + \sum_{i=1}^3 \Omega_{2c_i} \left(\frac{A_i}{A_{0n}} \right) \right] \exp\{\iota k_n x \sin \theta_n - \iota \omega t\}, \\ \psi &= A_{0n} \left[\Omega_{3c_n} + \sum_{i=1}^3 \Omega_{3c_i} \left(\frac{A_i}{A_{0n}} \right) \right] \exp\{\iota k_n x \sin \theta_n - \iota \omega t\}. \end{aligned}$$

(ii) For the incidence of shear wave having phase speed V_4 , we have

$$\begin{aligned} u &= \iota A_{04} \left[\sum_{i=1}^3 k_i \sin \theta_i \left(\frac{A_i}{A_{04}} \right) + \left(1 - \frac{A_4}{A_{04}} \right) k_4 \cos \theta_4 \right] \exp\{\iota k_4 x \sin \theta_4 - \iota \omega t\}, \\ w &= \iota A_{04} \left[\sum_{i=1}^3 k_i \cos \theta_i \left(\frac{A_i}{A_{04}} \right) + \left(1 + \frac{A_4}{A_{04}} \right) k_4 \sin \theta_4 \right] \exp\{\iota k_4 x \sin \theta_4 - \iota \omega t\}, \\ \phi &= A_{04} \left[\sum_{i=1}^3 \Omega_{2c_i} \left(\frac{A_i}{A_{04}} \right) \right] \exp\{\iota k_4 x \sin \theta_4 - \iota \omega t\}, \\ \psi &= A_{04} \left[\sum_{i=1}^3 \Omega_{3c_i} \left(\frac{A_i}{A_{04}} \right) \right] \exp\{\iota k_4 x \sin \theta_4 - \iota \omega t\}. \end{aligned}$$

It is clear that the surface response is functions of coordinate x , frequency ω angle of incidence θ_n as well as reflection coefficients for each type of incident wave.

Table 1 Numerical values of material parameters

Symbol	Value	Symbol	Value
λ	1.5×10^{10} Pa	μ	7.5×10^9 Pa
b	1×10^{10} Pa	d	1.2×10^{10} Pa
α	8×10^9 Pa m ²	b_1	7.9×10^6 Pa m ²
α_3	1.26×10^6 Pa	γ	8.2×10^9 Pa m ²
α_1	1.2×10^{10} Pa	α_2	2.21×10^{10} Pa
ρ	2×10^3 kg m ⁻³	χ_1	320 kg m ⁻¹
χ_2	330 kg m ⁻¹	e_0	0.39
τ_ϕ	1×10^6 Pa s	τ_ψ	1.2×10^6 Pa s
a	0.5×10^{-9} m	f	50 kHz

8 Numerical results and discussion

To study the behavior of reflection coefficients and corresponding energy ratios due to the incidence of coupled longitudinal waves/shear wave striking at the stress-free boundary of the half-space containing double voids, a hypothetical numerical model is considered. The numerical values of relevant material parameters have been borrowed from Puri and Cowin [6] and Eringen [35]. The parameters corresponding to the second type of voids are considered close to that of the first type of voids keeping in view that they must satisfy the required thermodynamical constraints. These values are listed in Table 1.

Figure 1 depicts the variation of reflection coefficients $|X_i|$, ($i = 1, 2, 3, 4$) with angle of incidence θ_3 in the range $0^\circ \leq \theta_3 \leq 90^\circ$ for the incidence of a set of coupled longitudinal waves having phase speed V_3 at $f = 50$ kHz for Voigt ($\tau_\phi \neq 0$, $\tau_\psi \neq 0$) and non-Voigt ($\tau_\phi = \tau_\psi = 0$) models. The coefficients $|X_1|$ and $|X_2|$ are depicted after magnifying by a factor of 15. The reflection coefficients $|X_1|$ and $|X_2|$ attain values 0.0239 and 0.0132, respectively, at normal incidence, and they remain almost constant up to $\theta_3 = 45^\circ$. Beyond $\theta_3 = 45^\circ$, there is a sudden increase in both the reflection coefficients and they attain their maximum value at $\theta_3 = 50.72^\circ$ and $\theta_3 = 50.95^\circ$, respectively. The sharp rise in the reflection coefficients is due to the appearance of critical angles in the considered numerical model. These critical angles arose due to the fact that the phase speed V_3 of incidence set of coupled longitudinal waves is found to be less than that of reflected sets of coupled waves with phase speeds V_1 and V_2 at the chosen frequency of 50 kHz. After their respective critical angles, these reflection coefficients decrease sharply and tend to zero as $\theta_3 \rightarrow 90^\circ$. The reflection coefficient $|X_3|$ starts with a maximum value of 1 at $\theta_3 = 0^\circ$ and decreases till the angle 64.63° to a value of 0.3827. Beyond $\theta_3 = 64.63^\circ$, the reflection coefficient $|X_3|$ starts increasing and tends to the value 1 at grazing incidence. Moreover, the reflection coefficient $|X_4|$ starts with zero value at normal incidence and increases with an increase in the angle of incidence θ_3 till $\theta_3 = 47.89^\circ$. After this, the value of $|X_4|$ starts decreasing and tends to zero at grazing incidence. It is clear from Fig. 1 that there is no comparable difference in the values of reflection coefficients for both Voigt and non-Voigt models.

Figure 2 depicts the variation of energy ratios $|E_i|$, ($i = 1, 2, 3, 4$) of reflected waves with respect to the angle of incidence θ_3 for both Voigt and non-Voigt models. The variations of $|E_i|$ are analogous to the corresponding reflection coefficients as was expected. It is shown numerically that the sum of all the absolute energy ratios remains unity in the considered range of the angle of incidence. This shows that there is no loss of energy at the boundary surface at each angle of incidence.

Figures 3, 4, 5 and 6 represent the variation of phase change Z_i , ($i = 1, 2, 3, 4$), associated with reflection coefficients, of reflected waves having phase speeds V_i , ($i = 1, 2, 3, 4$) with angle of incidence of coupled longitudinal waves having phase speed V_3 for the case of Voigt and non-Voigt models, respectively. It is observed from these figures that there is change in phase at the critical angles of reflected waves. It is also observed that in case of non-Voigt model, the change in phase of reflected waves is zero below the respective critical angles of reflected wave as these reflection coefficients are real-valued below their respective critical angles.

Figure 7 depicts the variation of reflection coefficients $|X_i|$, ($i = 1, 2, 3, 4$) with respect to the angle of incidence θ_4 due to incident transverse wave having phase speed V_4 at $f = 50$ kHz for both Voigt and non-Voigt models. The reflection coefficients $|X_1|$ and $|X_2|$ have been depicted after magnifying by a factor of 10^2 . In both models, the reflection coefficients $|X_1|$ and $|X_2|$ begin with the zero value at normal incidence and they increase slowly with angle of incidence and show a sharp rise in their values at 22.78° and 22.82° ,

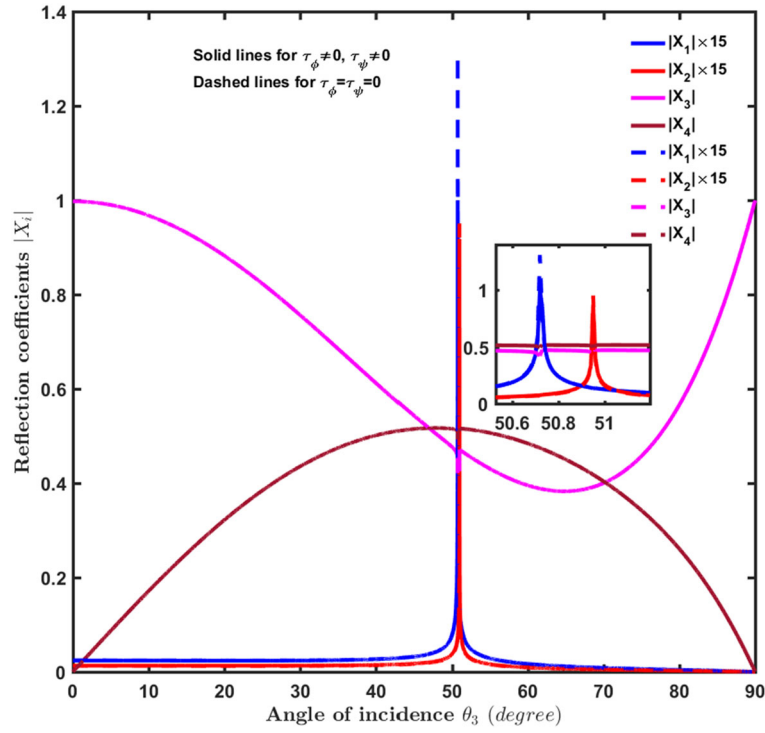


Fig. 1 Variation of reflection coefficients $|X_i|$ against the angle of incidence (θ_3) of coupled longitudinal waves having phase speed V_3 for Voigt ($\tau_\phi \neq 0, \tau_\psi \neq 0$) and non-Voigt ($\tau_\phi = \tau_\psi = 0$) models

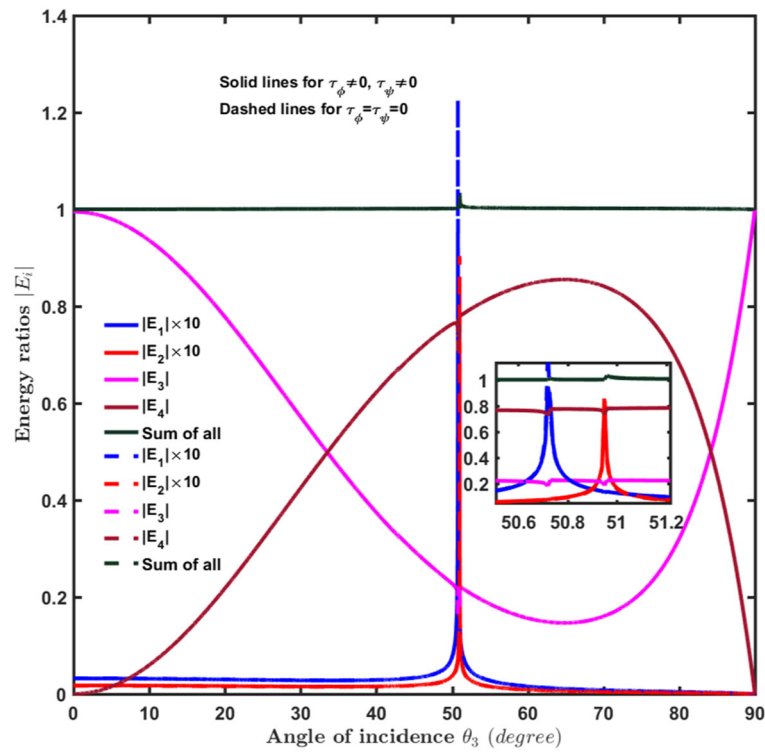


Fig. 2 Variation of energy ratios $|E_i|$ against the angle of incidence (θ_3) of coupled longitudinal waves having phase speed V_3 for Voigt ($\tau_\phi \neq 0, \tau_\psi \neq 0$) and non-Voigt ($\tau_\phi = \tau_\psi = 0$) models

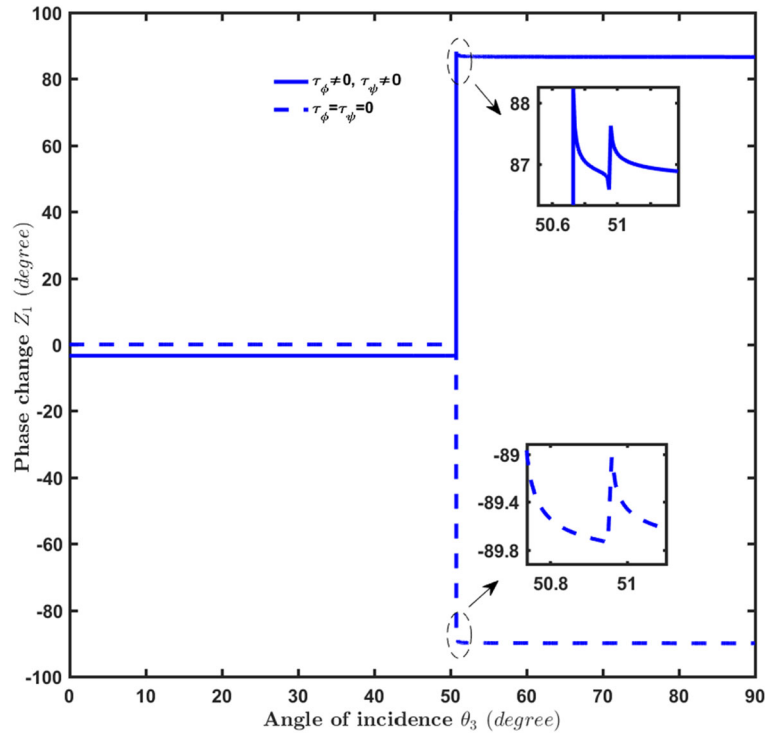


Fig. 3 Variation of phase change of reflected coupled longitudinal waves having phase speed V_1 with respect to angle of incidence (θ_3) for incident coupled longitudinal waves having phase speed V_3

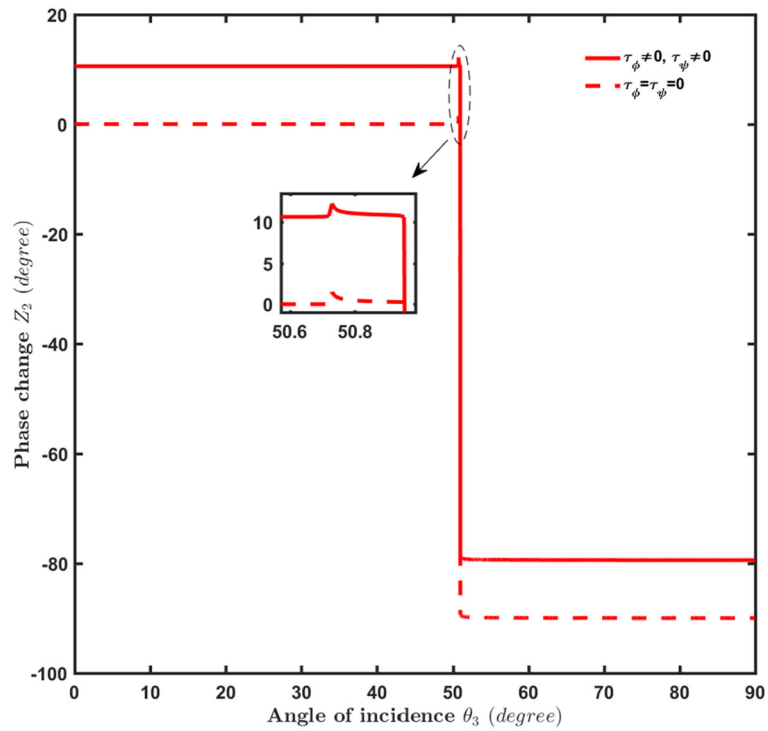


Fig. 4 Variation of phase change of reflected coupled longitudinal waves having phase speed V_2 with respect to angle of incidence (θ_3) for incident coupled longitudinal waves having phase speed V_3

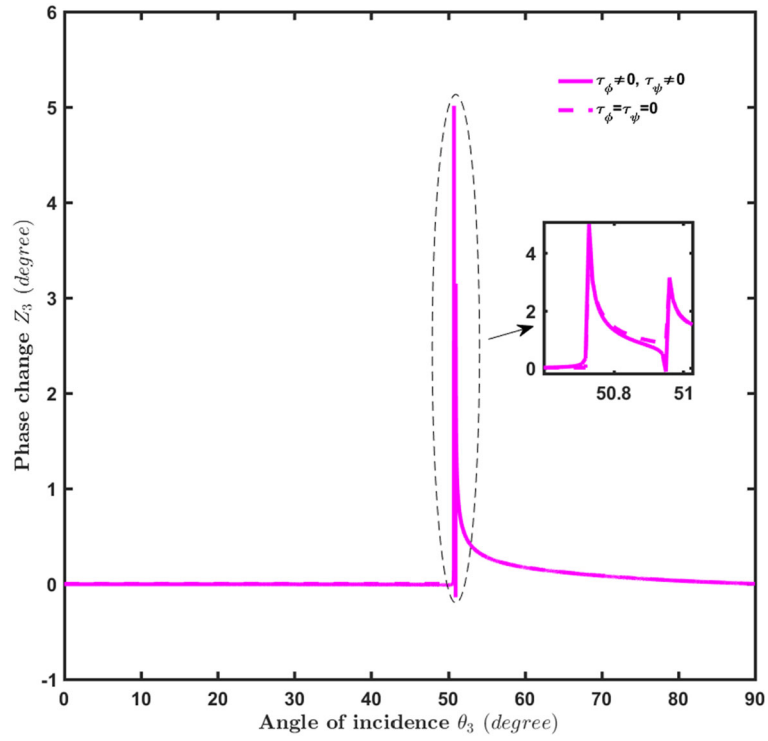


Fig. 5 Variation of phase change of reflected coupled longitudinal waves having phase speed V_3 with respect to angle of incidence (θ_3) for incident coupled longitudinal waves having phase speed V_3

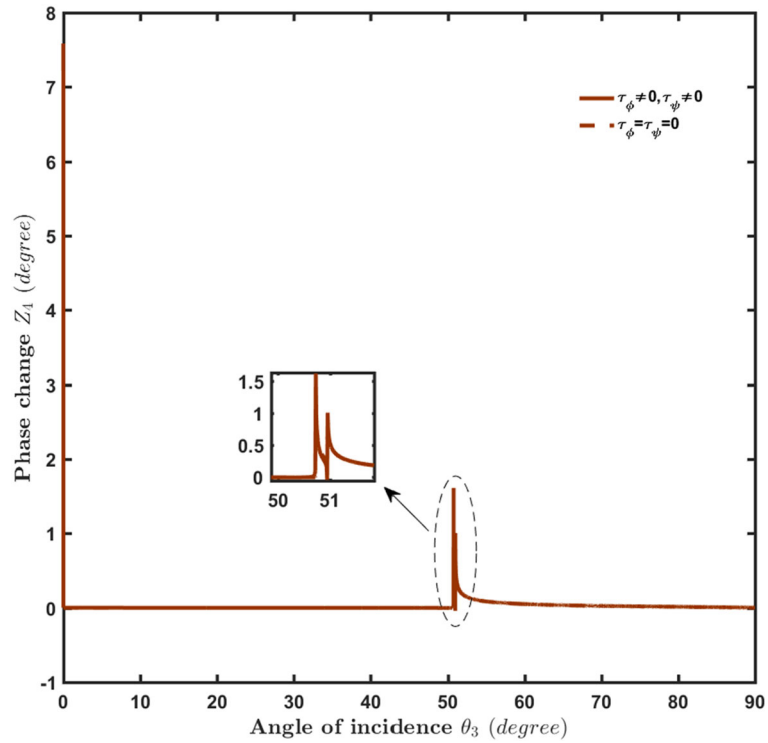


Fig. 6 Variation of phase change of reflected shear waves having phase speed V_4 with respect to angle of incidence (θ_3) for incident coupled longitudinal waves having phase speed V_3

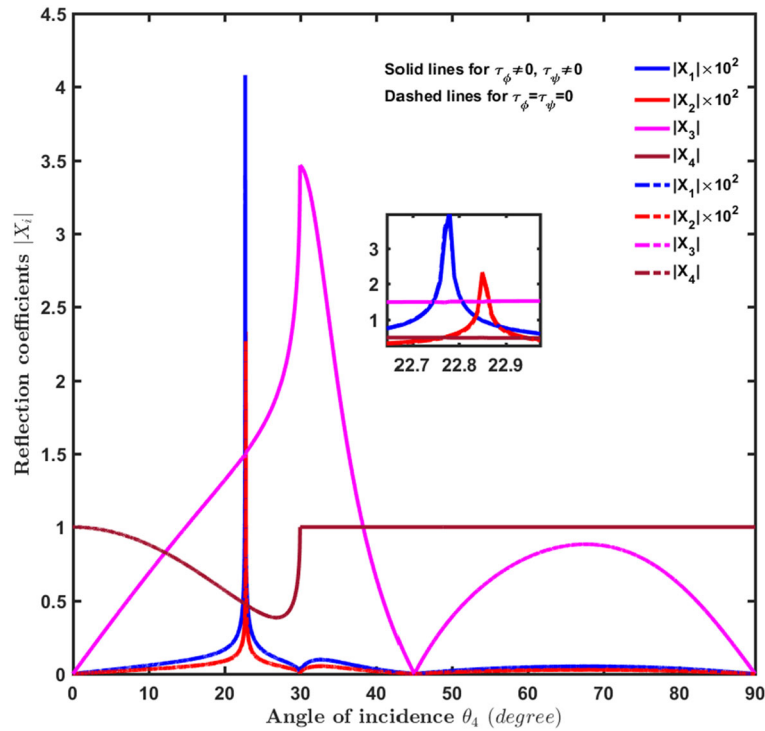


Fig. 7 Variation of reflection coefficients $|X_i|$ against the angle of incidence (θ_4) of shear wave having phase speed V_4 for Voigt ($\tau_\phi \neq 0, \tau_\psi \neq 0$) and non-Voigt ($\tau_\phi = \tau_\psi = 0$) models

respectively, due to the appearance of critical angles. Beyond their respective critical angles, $|X_1|$ and $|X_2|$ start decreasing and become close to zero at the angle $\theta_4 = 30.1^\circ$. Beyond $\theta_4 = 30.1^\circ$, their values start increasing slowly and increase up to $\theta_4 = 33.82^\circ$ and then decrease to almost zero at $\theta_4 = 45^\circ$, then again their values start increasing slowly and increases up to $\theta_4 = 67.28^\circ$. Beyond $\theta_4 = 67.28^\circ$ their values start decreasing and tend to zero at grazing incidence. The reflection coefficient $|X_3|$ shows a linearly increasing behavior in the range $0^\circ \leq \theta_4 \leq 27^\circ$ from a value 0 to a value of 1.903. Beyond $\theta_4 = 27^\circ$, its value increases rapidly to 3.465 at $\theta_4 = 30^\circ$. After this, $|X_3|$ starts decreasing and it decreases to zero at $\theta = 45^\circ$. After $\theta_4 = 45^\circ$, the value of reflection coefficient $|X_3|$ increases to 0.8828 at $\theta_4 = 68^\circ$ and then decreases to the zero value at $\theta_4 = 90^\circ$. The value of reflection coefficient $|X_4|$ starts from 1 at normal incidence and then decreases to 0.3828 at $\theta_4 = 26.99^\circ$. After $\theta_4 = 26.99^\circ$, its value starts increasing and increases to 1 at $\theta_4 = 30.01^\circ$. Beyond $\theta_4 = 30.01^\circ$, the value of reflection coefficient $|X_4|$ remains constant and have value equal to unity. Here, we note that there is no significant change in the values of reflection coefficients for Voigt and non-Voigt models.

Figure 8 depicts the behavior of energy ratios of reflected waves with the angle of incidence θ_4 of shear wave. We see that the behavior of absolute values of energy ratios is similar to the corresponding absolute values of reflection coefficients. From Fig. 9, it is shown that the sum of absolute values of all the energy ratios is unity. In another way, we can see that the sum of real parts of all the energy ratios is equal to unity and sum of the imaginary parts is zero which also verifies the conservation of energy method used by Ainslie and Burns [36], Singh and Tomar [37] and recently by Kumar and Tomar [31].

Figures 10, 11, 12 and 13 illustrate the behavior of phase change, associated with reflection coefficients, of reflected waves having phase Z_i , ($i = 1, 2, 3, 4$) of reflected waves having phase speed V_i , ($i = 1, 2, 3, 4$), respectively, with the angle of incidence of shear wave having phase speed V_4 for both Voigt and non-Voigt models. It is observed from these figures that there is change in phase of reflected waves at the critical angles. It is also observed that the phase change of all the reflected waves is zero below their respective critical angles in case of non-Voigt model.

Figures 14 and 15, respectively, represent the variation of reflection coefficients $|X_i|$, ($i = 1, 2, 3, 4$) and energy ratios $|E_i|$, ($i = 1, 2, 3, 4$) of all the reflected waves due to the incidence of coupled longitudinal waves having phase speed V_3 against the non-dimensional nonlocality parameter $\bar{\epsilon} = \epsilon k_\ell$, where $k_\ell = \frac{\omega}{c_\ell}$, at

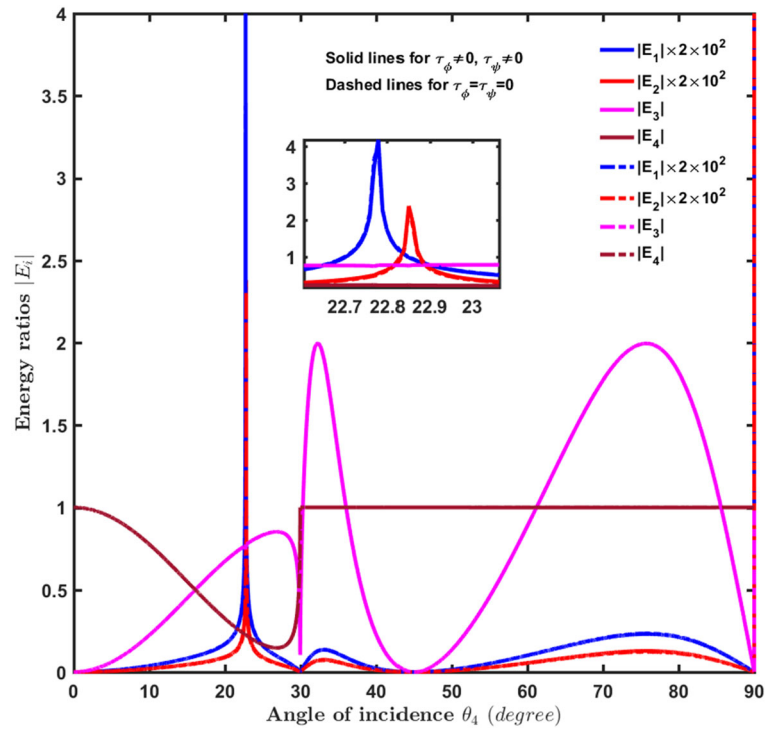


Fig. 8 Variation of energy ratios $|E_i|$ against the angle of incidence (θ_4) of shear wave having phase speed V_4 for Voigt ($\tau_\phi \neq 0$, $\tau_\phi \neq 0$) and non-Voigt ($\tau_\phi = \tau_\phi = 0$) models

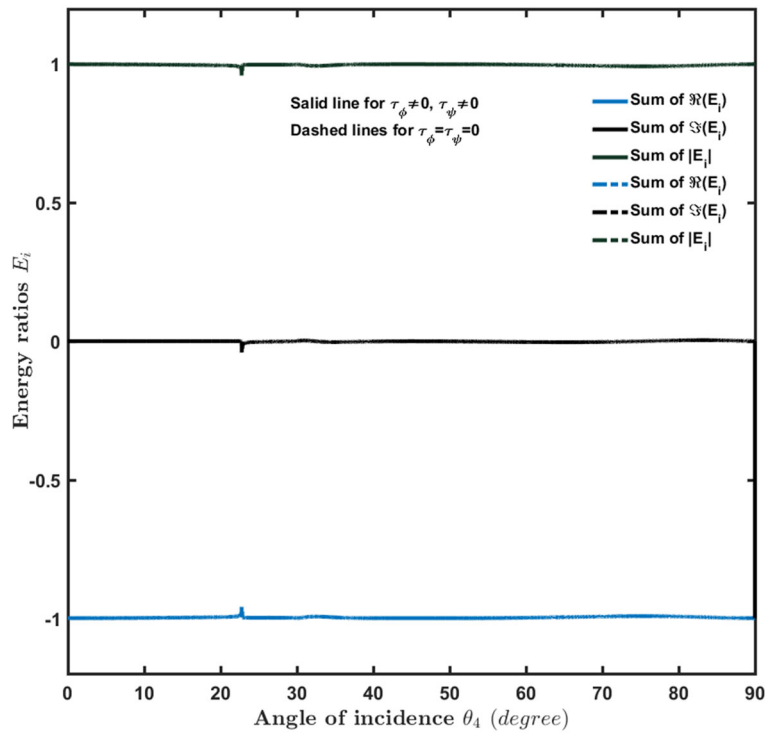


Fig. 9 Variation of sum of real, imaginary parts and absolute values of energy ratios E_i versus angle of incidence (θ_4) of shear wave having phase speed V_4 for Voigt ($\tau_\phi \neq 0$, $\tau_\phi \neq 0$) and non-Voigt ($\tau_\phi = \tau_\phi = 0$) models

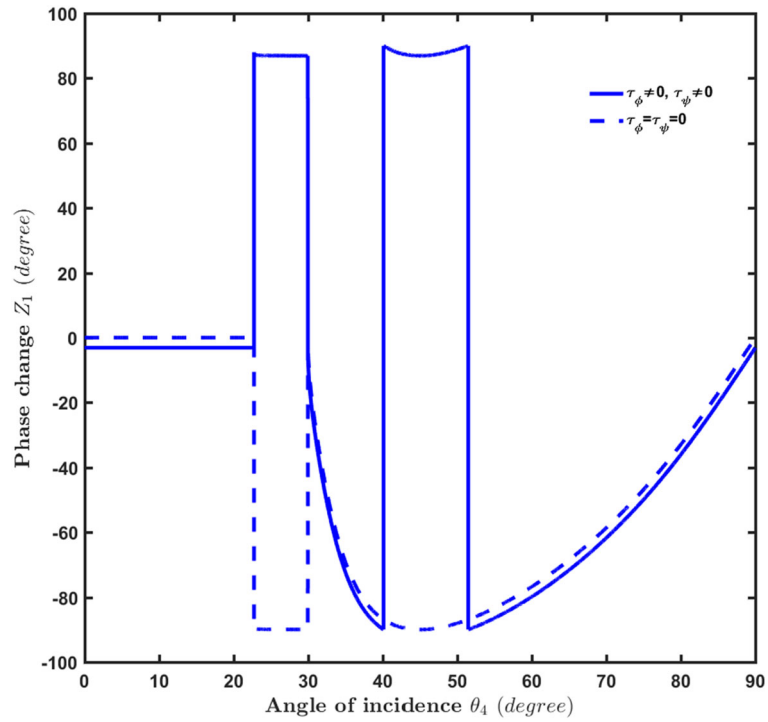


Fig. 10 Variation of phase change of reflected coupled longitudinal waves having phase speed V_1 with respect to angle of incidence (θ_4) for incident shear wave having phase speed V_4

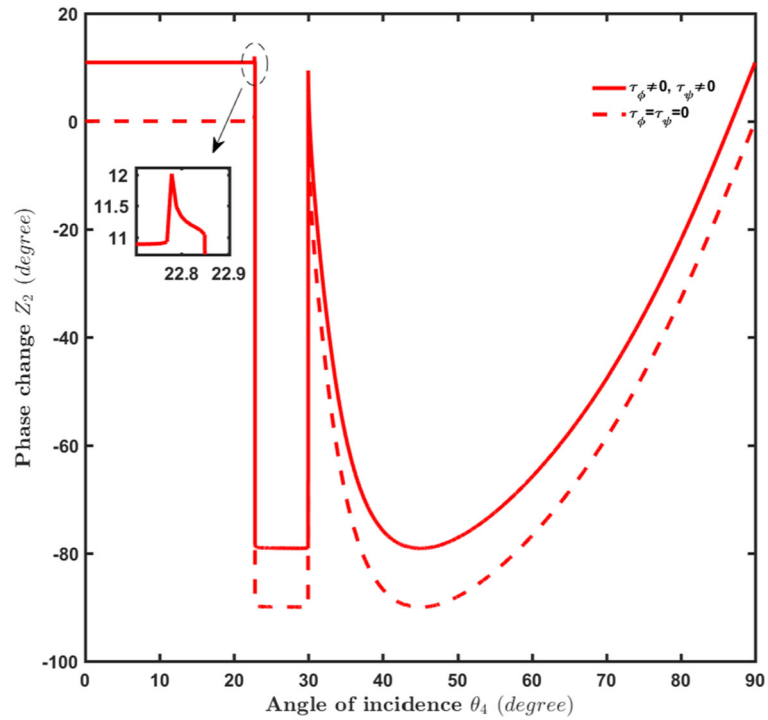


Fig. 11 Variation of phase change of reflected coupled longitudinal waves having phase speed V_2 with respect to angle of incidence (θ_4) for incident shear wave having phase speed V_4

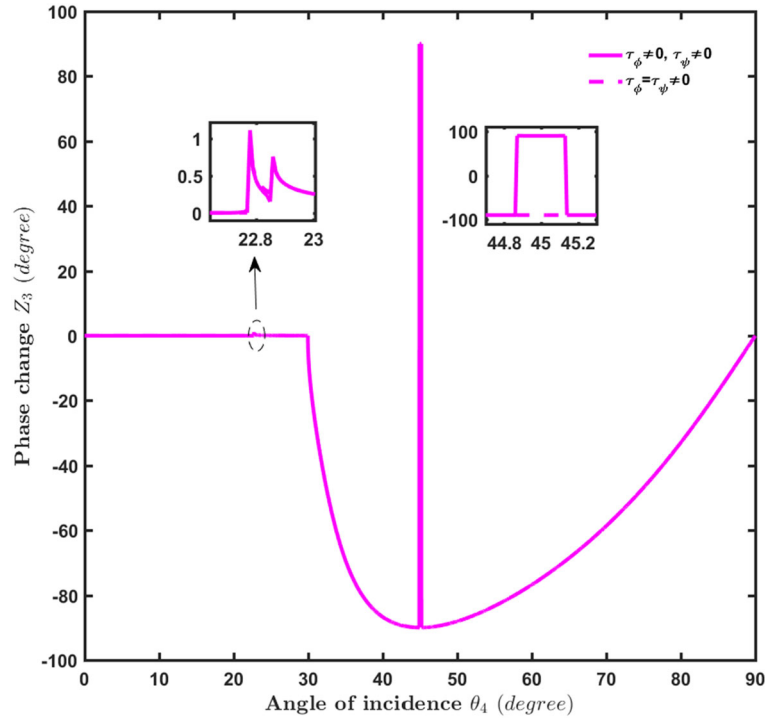


Fig. 12 Variation of phase change of reflected coupled longitudinal waves having phase speed V_3 with respect to angle of incidence (θ_4) for incident shear wave having phase speed V_4

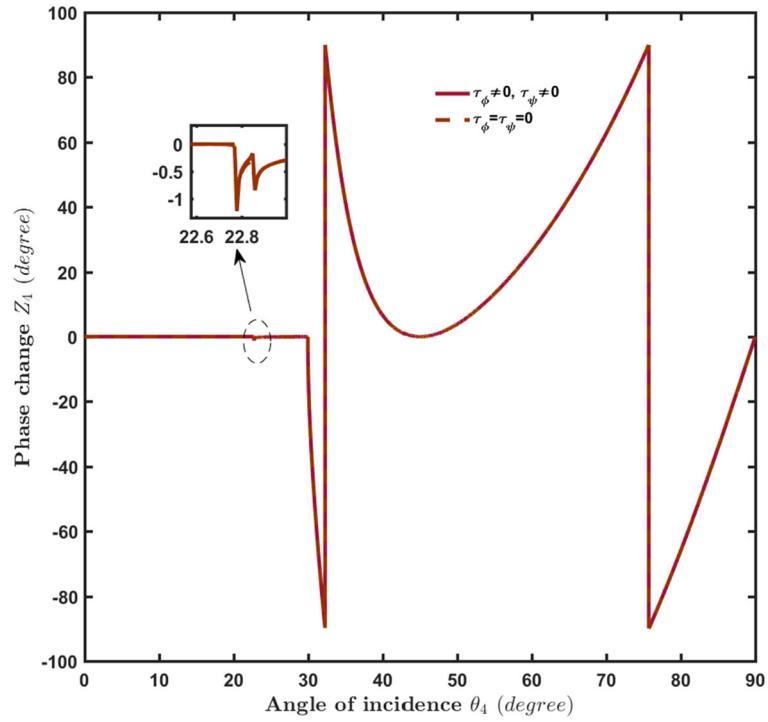


Fig. 13 Variation of phase change of reflected shear wave having phase speed V_4 with respect to angle of incidence (θ_4) for incident shear wave having phase speed V_4

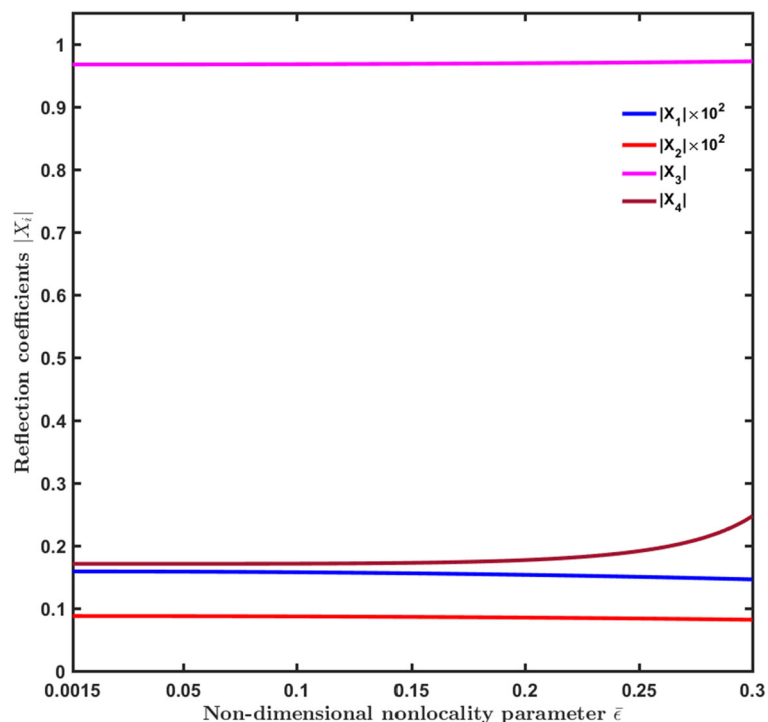


Fig. 14 Variation of reflection coefficients $|X_i|$ against nonlocality parameter ($\bar{\epsilon}$) for incident coupled longitudinal waves having phase speed V_3 at $\theta_3 = 10^\circ$

an angle of $\theta_3 = 10^\circ$ at $f = 50$ kHz having a range between $1.5 \times 10^{-3} < \bar{\epsilon} < 3 \times 10^{-1}$. The reflection coefficients $|X_1|$, $|X_2|$ and $|X_3|$ are poorly influenced by the parameter $\bar{\epsilon}$, while the values of coefficient $|X_4|$ is strongly affected by the nonlocal parameter. The value of reflection coefficient $|X_3|$ is found to be equal to 0.9675 at $\bar{\epsilon} = 1.5 \times 10^{-3}$ and then increases slightly to the value 0.9725 at $\bar{\epsilon} = 3 \times 10^{-1}$. The value of reflection coefficient $|X_4|$ starts from 0.171 at $\bar{\epsilon} = 1.5 \times 10^{-3}$ and its value remains almost constant up to the value $\bar{\epsilon} = 1 \times 10^{-1}$. Thereafter, its value starts increasing and increases to the value 0.2472 at 3×10^{-1} . We also note that the reflection coefficients $|X_1|$, $|X_2|$ show a decreasing behavior, while the reflection coefficients $|X_3|$ and $|X_4|$ show an increasing behavior with nonlocal parameter $\bar{\epsilon}$. It is clear from Fig. 15 that the behavior of energy ratios is almost similar to the corresponding reflection coefficients. During the variation of nonlocal parameter, the sum of all energy ratios is found to be equal to unit satisfying law of conservation of energy at the boundary surface.

Figures 16 and 17 depict the variation of reflection coefficients and corresponding energy ratios versus $\bar{\epsilon}$ for the case of incidence of shear wave having speed V_4 at an angle $\theta_4 = 5^\circ$ at $f = 50$ kHz. In the above considered range of non-dimensional nonlocality parameter, all the reflection coefficients show decreasing behavior. The value of $|X_1|$ decreases from 2.8×10^{-4} to 1.799×10^{-4} , while the value of $|X_2|$ decreases from 1.5×10^{-4} to 1.0×10^{-4} in the considered range of nonlocality. Similarly, the reflection coefficient $|X_3|$ decreases from 0.3469 to 0.2415, while the reflection coefficient $|X_4|$ is slightly influenced by the nonlocality in considered range. In this range, its value decreases slightly from 0.969 to 0.964. From Fig. 17, we can see that the behavior of all energy ratios $|E_1|$, $|E_2|$, $|E_3|$ and $|E_4|$ is similar to their respective reflection coefficients. One can note from Figs. 15 and 17 that the sum of energies of all the reflected waves is not unity for high values of non-dimensional nonlocality parameter. This is due to the fact that the approximation $(1 - \epsilon^2 \nabla^2)^{-1} \approx (1 + \epsilon^2 \nabla^2)$ has been used in the study.

Figures 18, 19, 20, 21 and 22 depict the variation of $|X_i|$, ($i = 1, 2, 3, 4$) with respect to the void parameters b , b_1 , α_3 , γ and α ranging between $1 \times 10^9 \text{ Pa} \leq b \leq 1.4 \times 10^{10} \text{ Pa}$, $5 \times 10^4 \text{ Pa m}^2 \leq b_1 \leq 8 \times 10^7 \text{ Pa m}^2$, $5 \times 10^4 \text{ Pa} \leq \alpha_3 \leq 1.5 \times 10^{10} \text{ Pa}$, $8 \times 10^9 \text{ Pa m}^2 \leq \gamma \leq 4 \times 10^{10} \text{ Pa m}^2$ and $8 \times 10^9 \text{ Pa m}^2 \leq \alpha \leq 4 \times 10^{10} \text{ Pa m}^2$, respectively, for the case of incidence of coupled longitudinal waves having phase speed V_3 at $f = 50$ kHz and $\theta_3 = 20^\circ$. We note that the values of reflection coefficients $|X_1|$ and $|X_2|$ are very small, while the values of reflection coefficients $|X_3|$ and $|X_4|$ are almost constant with respect to all the considered void parameters. Hence, the reflection coefficients are not much influenced by these void parameters.

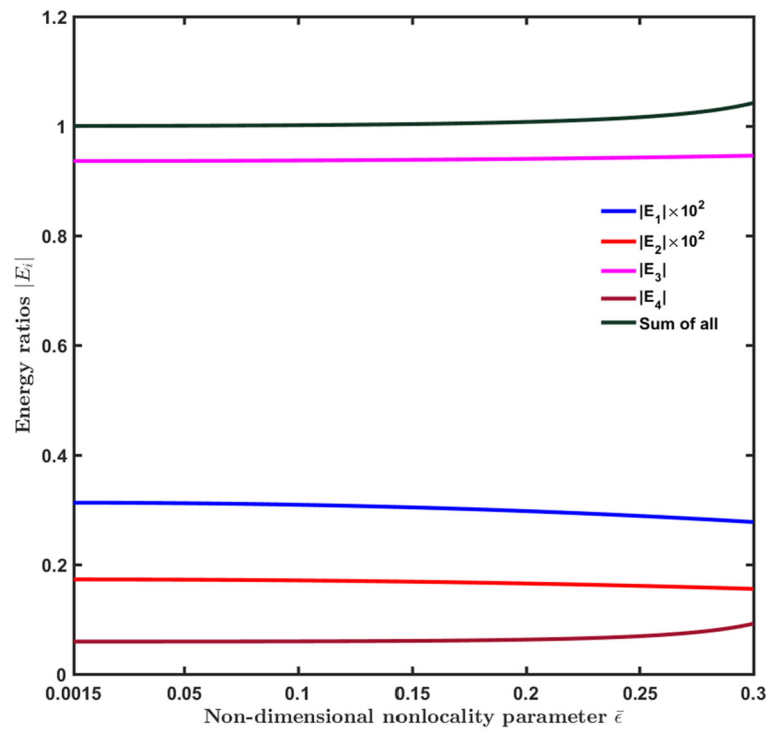


Fig. 15 Variation of energy ratios $|E_i|$ against nonlocality parameter ($\bar{\epsilon}$) for incident coupled longitudinal waves having phase speed V_3 at $\theta_3 = 10^\circ$

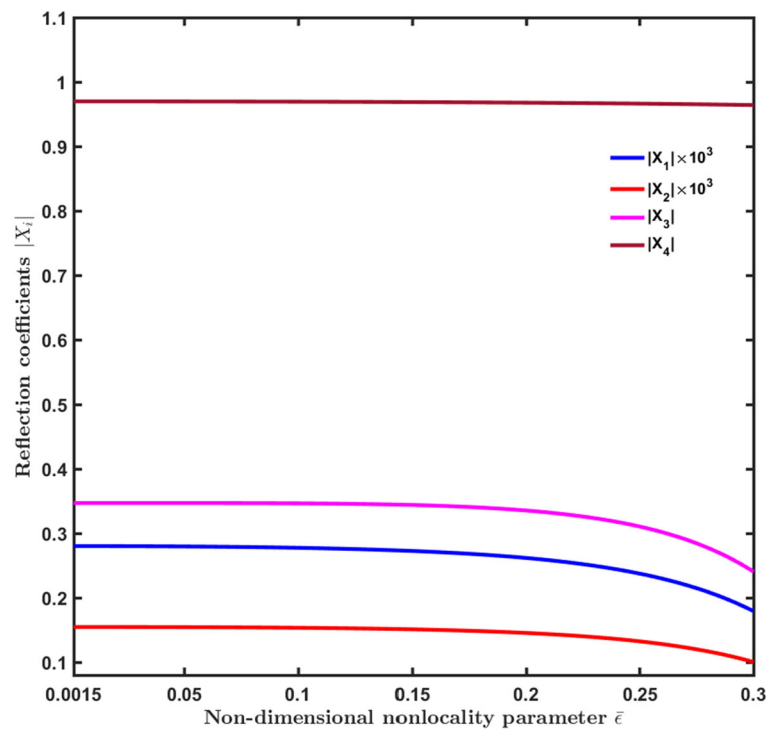


Fig. 16 Variation of reflection coefficients $|X_i|$ against nonlocality parameter ($\bar{\epsilon}$) for incident shear wave having phase speed V_4 at $\theta_4 = 5^\circ$

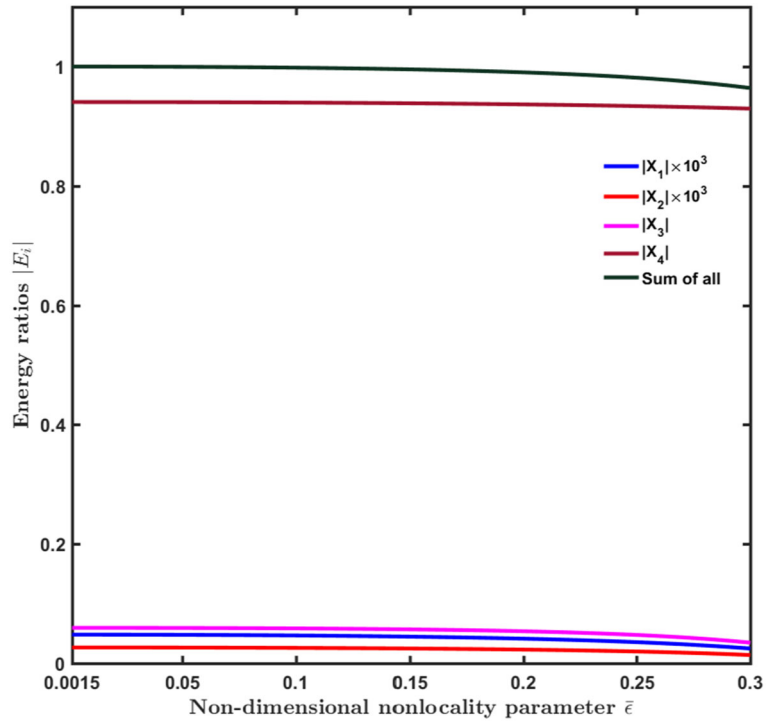


Fig. 17 Variation of energy ratios $|E_i|$ against nonlocality parameter ($\bar{\epsilon}$) for incident shear wave having phase speed V_4 at $\theta_4 = 5^\circ$

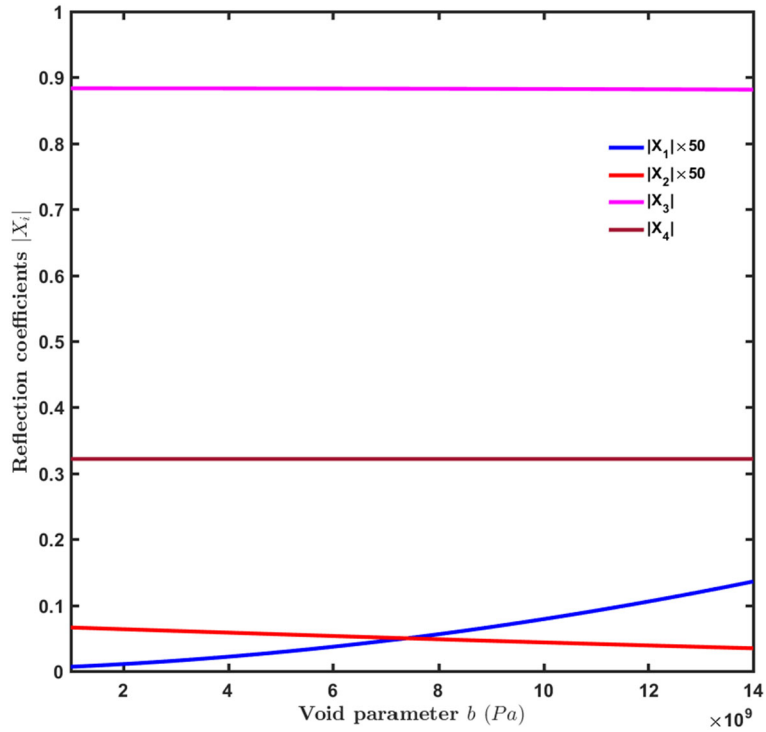


Fig. 18 Variation of reflection coefficients $|X_i|$ against void parameter (b) for incident coupled longitudinal waves having phase speed V_3 at $\theta_3 = 20^\circ$

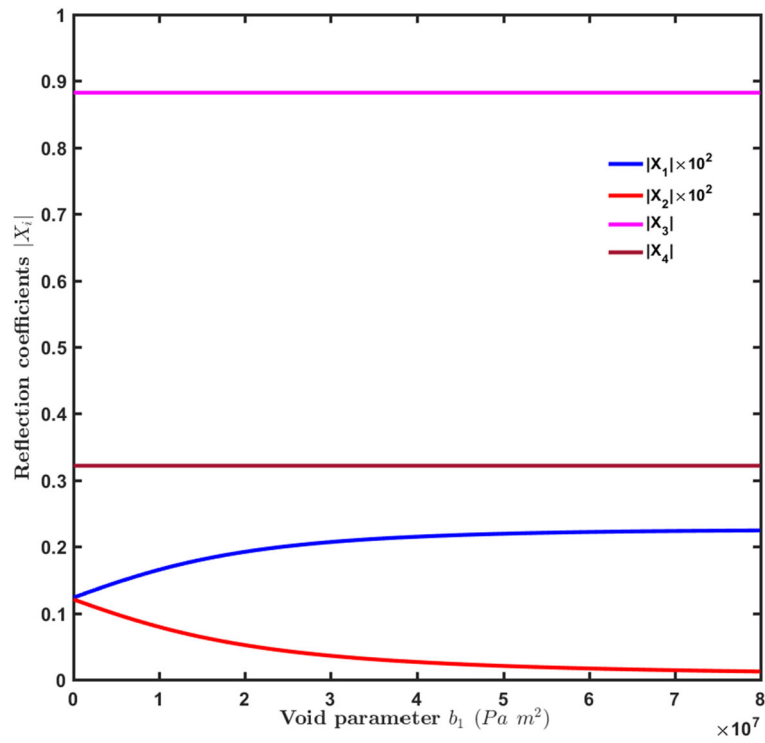


Fig. 19 Variation of reflection coefficients $|X_i|$ against void parameter (b_1) for incident coupled longitudinal waves having phase speed V_3 at $\theta_3 = 20^\circ$

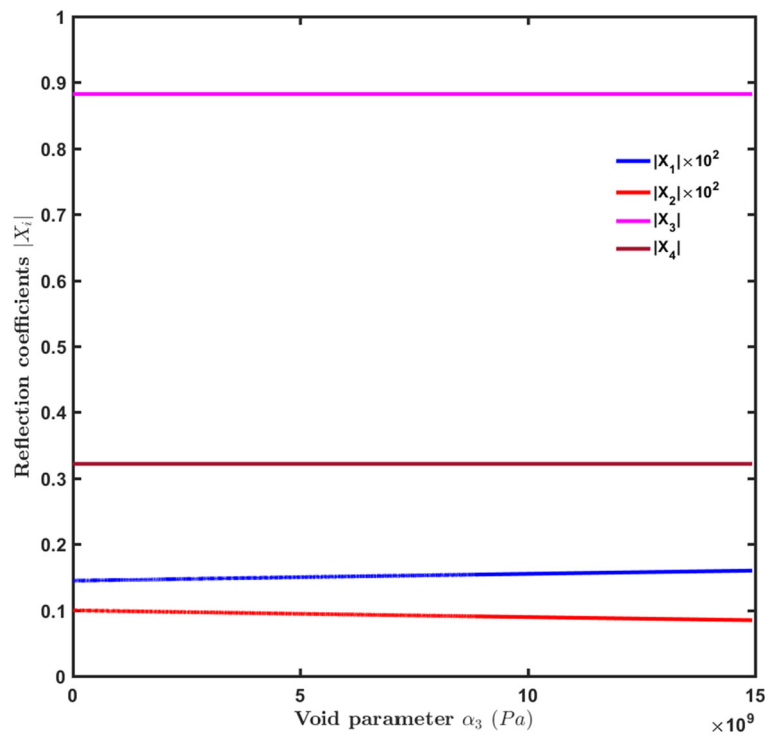


Fig. 20 Variation of reflection coefficients $|X_i|$ against void parameter (α_3) for incident coupled longitudinal waves having phase speed V_3 at $\theta_3 = 20^\circ$

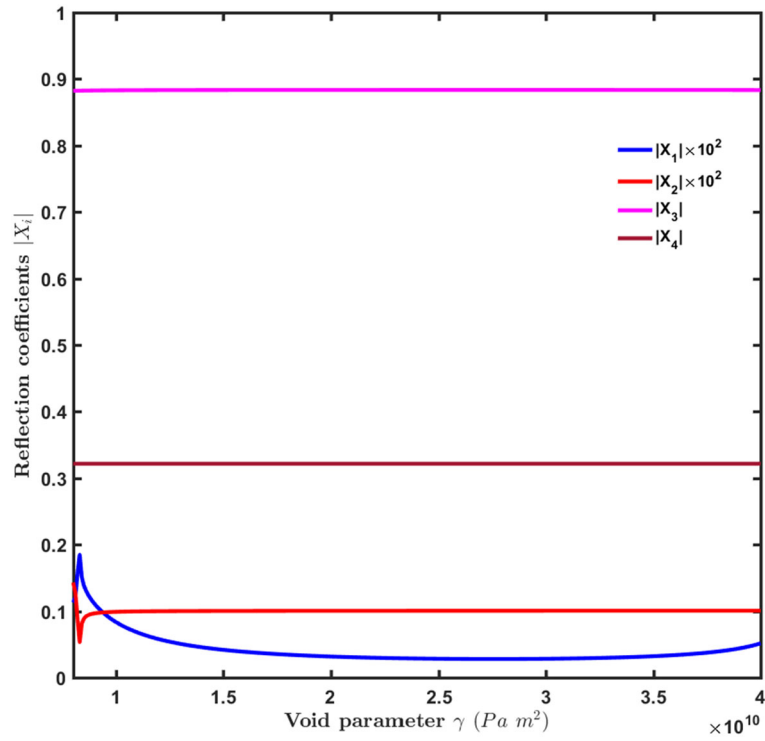


Fig. 21 Variation of reflection coefficients $|X_i|$ against void parameter (γ) for incident coupled longitudinal waves having phase speed V_3 at $\theta_3 = 20^\circ$

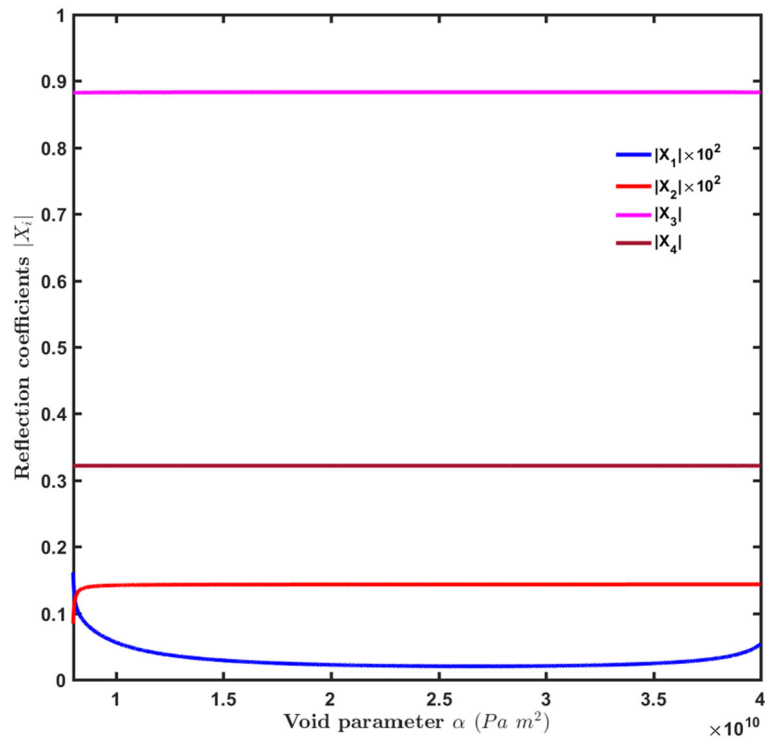


Fig. 22 Variation of reflection coefficients $|X_i|$ against void parameter (α) for incident coupled longitudinal waves having phase speed V_3 at $\theta_3 = 20^\circ$

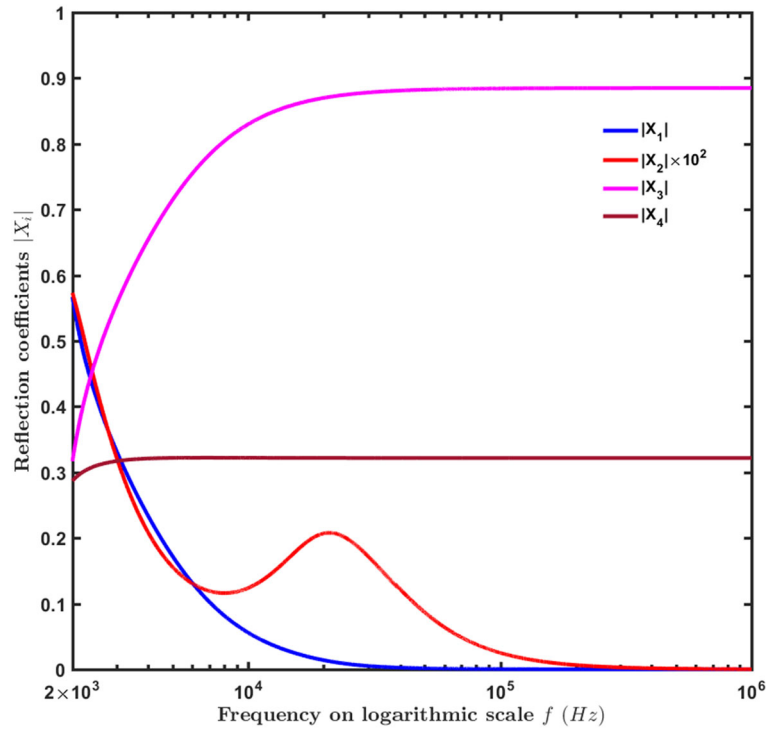


Fig. 23 Variation of reflection coefficients $|X_i|$ against frequency (f) on logarithmic scale for incident coupled longitudinal waves having phase speed V_3 at $\theta_3 = 20^\circ$

Figure 23 depicts the variation of reflection coefficients $|X_i|$, ($i = 1, 2, 3, 4$) at an angle of $\theta_3 = 20^\circ$ with respect to the frequency parameter f on logarithmic scale ranging between $2 \times 10^3 \text{ Hz} \leq f \leq 10^6 \text{ Hz}$ for the case of incidence of coupled longitudinal waves having phase speed V_3 . We see that the value of reflection coefficient $|X_1|$ decreases with an increase in linear frequency. It starts with a value 0.5663 at $f = 2 \times 10^3 \text{ Hz}$ and then decreases to the zero value at $f = 8 \times 10^4 \text{ Hz}$, and it remains zero afterward. The value of coefficient $|X_2|$ is found to be very small in magnitude, and therefore it has been depicted after multiplying by a factor of 10^2 . The coefficient $|X_2|$ has a value of 5.728×10^{-3} at $f = 2 \times 10^3 \text{ Hz}$; thereafter, it starts decreasing and attains the value 1.161×10^{-3} at $f = 8160 \text{ Hz}$. After this, it starts increasing and reaches to 2.079×10^{-3} at $f = 2.1 \times 10^4 \text{ Hz}$. Beyond $f = 2.1 \times 10^4 \text{ Hz}$, it starts decreasing and tends to zero for further increase in value of frequency. The value of reflection coefficient $|X_3|$ is found to be equal to 0.32 at $f = 2 \times 10^3 \text{ Hz}$ and it increases to 0.8824 at $f = 5 \times 10^4 \text{ Hz}$. Beyond $f = 5 \times 10^4 \text{ Hz}$, $|X_3|$ remains almost constant. The reflection coefficient $|X_4|$ starts with a value of 0.2869 at $f = 2 \times 10^3 \text{ Hz}$ and increases to 0.3201 at $f = 3.630 \times 10^3 \text{ Hz}$. Beyond this, it remains almost constant like $|X_3|$.

Figures 24 and 25 depict the variation of absolute values of normalized surface displacements u , w and change in void fractional fields ϕ , ψ , respectively, with respect to the angle of incidence for coupled dilatational waves having phase speed V_3 . Here, the absolute values of u , w have been normalized by the absolute value of w at normal incidence. It is found that the normalized value of vertical displacement w starts decreasing from unity with an increase in the angle of incidence and it tends to zero for grazing incidence. While the value of horizontal displacement u starts increasing from zero and tends to maximum value to 0.6993 at $\theta_3 = 58.81^\circ$, thereafter it tends to zero at grazing incidence. It is also observed from Fig. 24 that there is a slight decrease in the values of displacements at angles 50.72° and 50.95° . This is due to the critical angles faced by the reflected waves corresponding to phase speed V_1 and V_2 , respectively. In Fig. 25, the values of ϕ , ψ have been normalized with the absolute value of ϕ at normal incidence. It is observed that the normalized value of ϕ starts from unity and remains almost constant up to 44° , then there is sharp rise and goes to the maximum value 36.05 at critical angle 50.72° . Thereafter, it tends to value 0.5583 at grazing incidence. A similar behavior is also observed for ψ , it starts from value of 1.18, then increases to the maximum value 42.47 near the critical angle 50.95° , and then ultimately tends to the value 0.32 as $\theta_3 \rightarrow 90^\circ$.

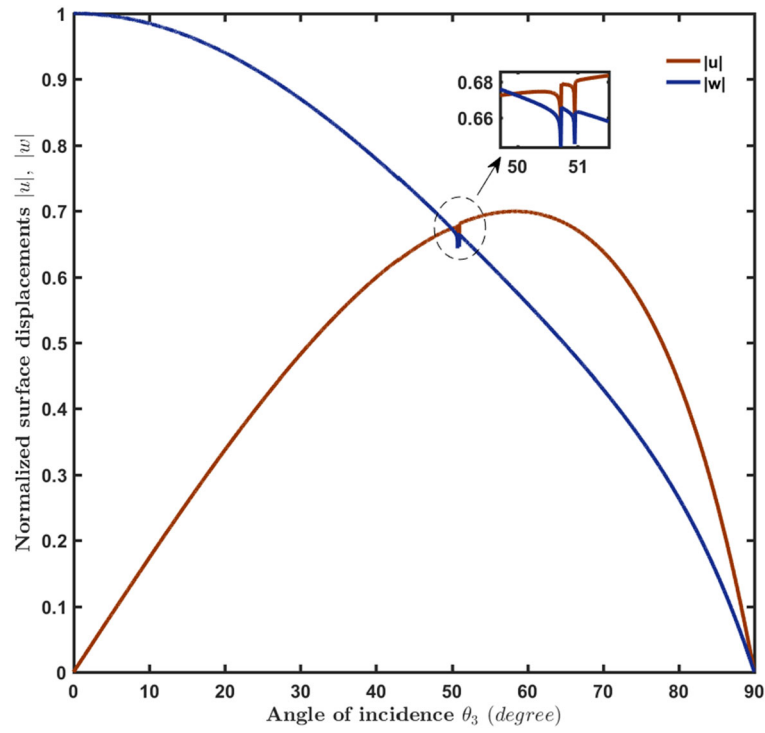


Fig. 24 Variation of absolute value of normalized surface displacements $|u|$, $|w|$ with respect to angle of incidence (θ_3) for incident coupled longitudinal waves having phase speed V_3

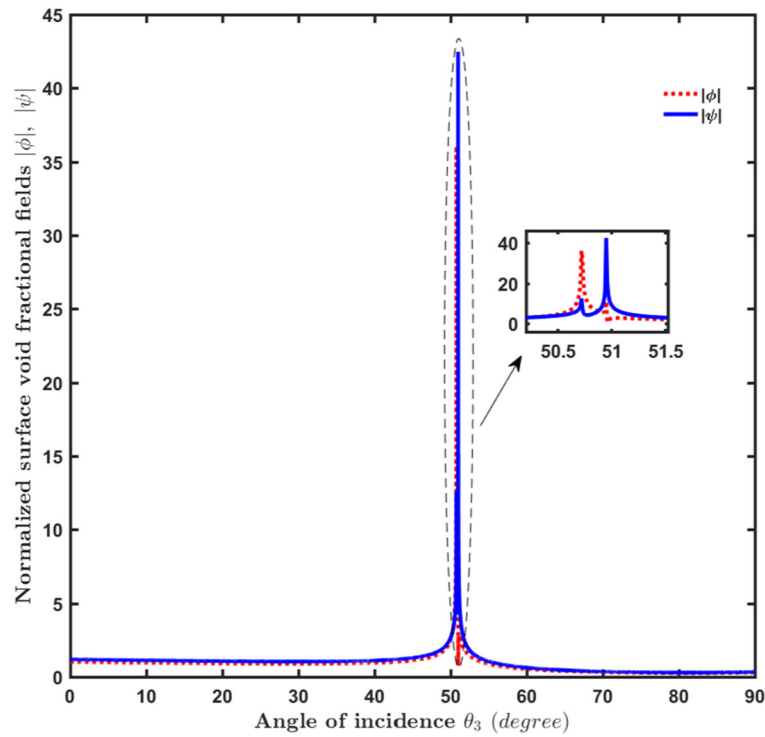


Fig. 25 Variation of absolute value of normalized surface void fractional fields $|\phi|$, $|\psi|$ with respect to angle of incidence (θ_3) for incident coupled longitudinal waves having phase speed V_3

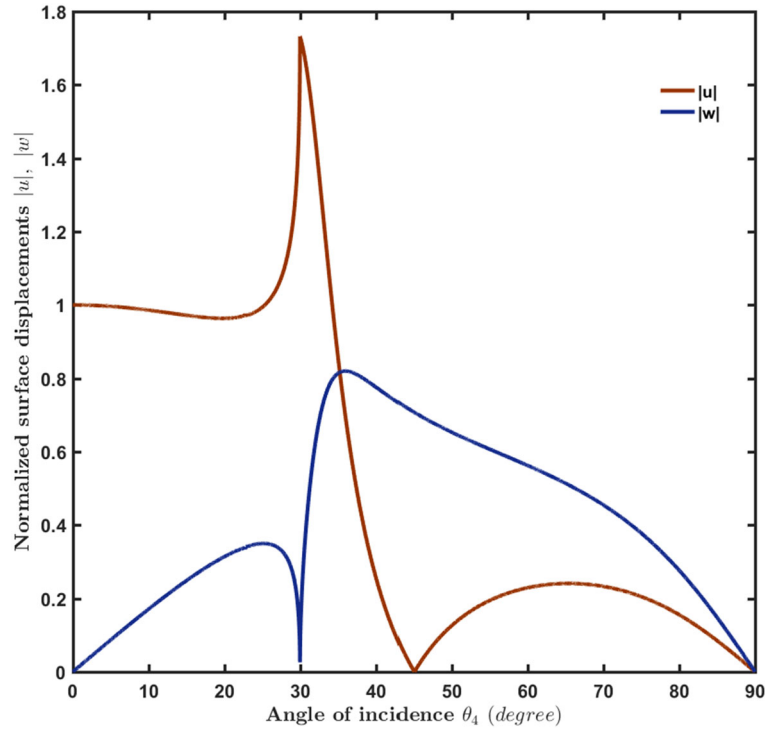


Fig. 26 Variation of absolute value of normalized surface displacements $|u|$, $|w|$ with respect to angle of incidence (θ_4) for incident shear wave having phase speed V_4

Figures 26 and 27 depict the variation of absolute values of normalized surface displacements u , w , and void fractional fields ϕ , ψ , respectively, with respect to the angle of incidence of shear wave having phase speed V_4 . Here, the values of u , w have been normalized by the absolute value of u at normal incidence and the values of ϕ , ψ have been normalized with the absolute value of ϕ at normal incidence. It is observed that the horizontal displacement u starts from unity and then slightly decreases to 0.9635 at 20.01°; thereafter, its value increases to 1.732 as angle of incidence tends to 30.02°. Thereafter, it tends to zero value at 45° and then starts increasing to the value 0.2408 at 65.95°. Beyond 65.95°, it decreases to zero at grazing incidence. The value of vertical displacement w starts increasing from zero to the value 0.3495 at an angle 25.47° and then decreases to 0.025 at 30.01°. Beyond 30.01°, it increases sharply to the value 0.8199 at 36.09° and then decreases to zero at grazing incidence. From Fig. 27, it is observed that the normalized value of ϕ starts from unity and increases slowly up to 20°, then shows a sharp rise to the maximum value 80.35 at the angle 22.78°. Beyond 22.78°, it decreases to value 1.697 at 29.86°, and then increases to the value 2.351 at 32.22°. Thereafter, its value tends to unity at grazing incidence. Similarly, the value of ψ starts from 1.182 and then shows a maximum value 60.31 at 22.85°. Beyond this, the value decreases to 1.004 at 29.89°, then it increases to the value 2.786 at 32.28°, thereafter its value decreases to 1.182 at grazing incidence.

9 Conclusions

In the present paper, we have studied the reflection phenomena of plane waves from the stress-free boundary surface of a linear nonlocal homogeneous and isotropic elastic solid half-space having double porosity structure. Employing nonlocal stress-free boundary conditions, the reflection coefficients for the incidence of coupled longitudinal waves having phase speed V_n , ($n = 1, 2, 3$) and shear wave having phase speed V_4 are obtained. The following conclusions can be inferred from this study.

1. All the reflection coefficients depend on nonlocality of the medium, void parameters, angle of incidence, frequency of the incident wave and material moduli.

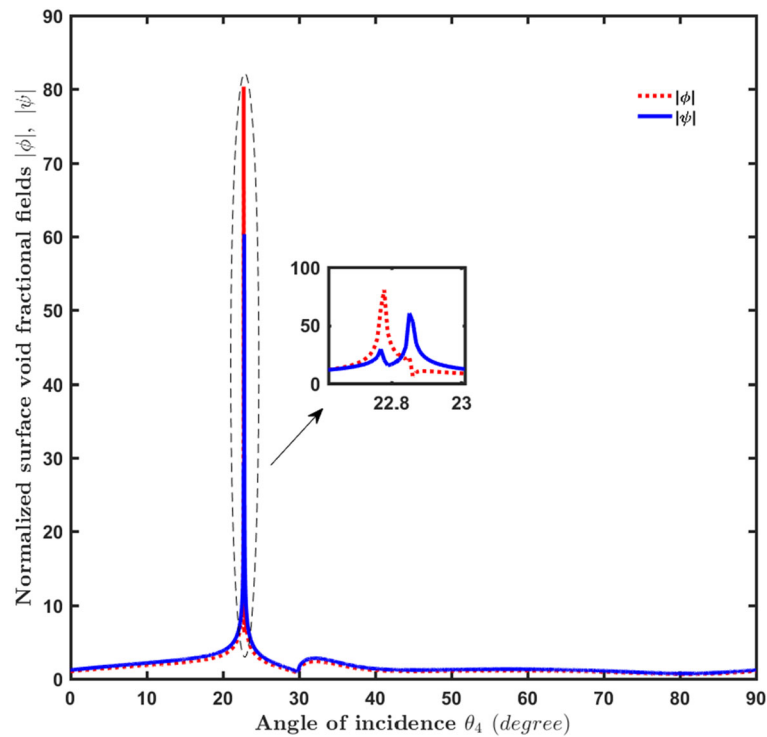


Fig. 27 Variation of absolute value of normalized surface void fractional fields $|\phi|$, $|\psi|$ with respect to angle of incidence (θ_4) for incident shear wave having phase speed V_4

2. The maximum amount of the incident energy goes along that reflected wave, which travels with the same speed as that of the incident wave for initial range of angles, irrespective of whether the incident wave is coupled longitudinal waves or shear wave.
3. The reflected waves, which is predominantly corresponding to the change in void volume fraction of the first and second kind of voids, face critical angles in both the cases of incidence.
4. The reflection coefficient corresponding to the incident wave remains almost the same in the considered range of $\bar{\epsilon}$ in both the cases.
5. In case of incident coupled longitudinal waves with phase velocity V_3 , the reflection coefficient $|X_4|$ shows an increasing behavior with nonlocal parameter $\bar{\epsilon}$, while the coefficients $|X_1|$ and $|X_2|$ remain almost constant.
6. In case of incident shear wave, the reflection coefficients $|X_1|$, $|X_2|$ and $|X_3|$ decrease with nonlocal parameter $\bar{\epsilon}$.
7. All the reflection coefficients are found to be influenced poorly by void parameters b , b_1 , α_3 , γ and α in case of incidence of coupled longitudinal waves propagating with phase velocity V_3 .
8. The sum of energy ratios corresponding to various reflected waves is found to be unity in all the cases of incidence. This shows that there is no dissipation of energy at boundary surface for each angle of incidence.
9. It is found that there is a phase shift in the reflected waves, who face critical angles. Also, in case of non-dissipative (dissipative) model, the phase change is zero (nonzero) below the respective critical angles for reflected coupled longitudinal waves.

The double porosity continua have applications in manmade materials, geophysics, mathematical biology, seismology, nuclear waste treatment, nuclear material behavior, study of lava from Mount Etna and many other engineering branches (see Straughan [17]).

Acknowledgements The authors are thankful to DST, New Delhi, and JSPS for providing funds under DST-JSPS project sanctioned to Sushil K. Tomar and Sohichi Hirose through Grant Nos. DST/INT/JSPS/P-322/2020 and JPJSBP-120207707.

Open Access This article is licensed under a Creative Commons Attribution 4.0 International License, which permits use, sharing, adaptation, distribution and reproduction in any medium or format, as long as you give appropriate credit to the original author(s) and the source, provide a link to the Creative Commons licence, and indicate if changes were made. The images or other

third party material in this article are included in the article's Creative Commons licence, unless indicated otherwise in a credit line to the material. If material is not included in the article's Creative Commons licence and your intended use is not permitted by statutory regulation or exceeds the permitted use, you will need to obtain permission directly from the copyright holder. To view a copy of this licence, visit <http://creativecommons.org/licenses/by/4.0/>.

Author contribution DK, DS and SKT contributed to conceptualization, methodology, and writing—original draft preparation; DK and DS performed formal analysis and investigation; SH, TS, AF and TM contributed to writing—review and editing; SKT and SH contributed to funding acquisition and supervision.

Declarations

Conflict of interest The authors declare that they have no conflict of interest.

References

- Ewing, W.M., Jardetzky, W.S., Press, F.: *Elastic Waves in Layered Media*. Mc-Graw-Hill Book Company Inc, New York (1957)
- Achenbach, J.D.: *Wave Propagation in Elastic Solids*. North Holland Publishing Co., New York (1973)
- Aki, K., Richards, P.G.: *Quantitative Seismology*, 2nd Ed., *University Science Books*, (2002)
- Nunziato, J.W., Cowin, S.C.: A non-linear theory of elastic materials with voids. *Arch. Ration. Mech. Anal.* **72**(2), 175–201 (1979)
- Cowin, S.C., Nunziato, J.W.: Linear elastic materials with voids. *J. Elast.* **13**(2), 125–147 (1983)
- Puri, P., Cowin, S.C.: Plane waves in linear elastic materials with voids. *J. Elast.* **15**(2), 167–183 (1985)
- Ciarletta, M., Sumbatyan, M.A.: Reflection of the plane waves by the free boundary of a porous elastic half-space. *J. Sound Vib.* **259**(2), 253–264 (2003)
- İeşan, D.: A theory of thermoelastic materials with voids. *Acta Mech.* **60**(1–2), 67–89 (1986)
- İeşan, D., Quintanilla, R.: On a theory of thermoelastic materials with a double porosity structure. *J. Therm. Stress.* **37**(9), 1017–1036 (2014)
- Svanadze, M.: Plane waves, uniqueness theorems and existence of eigen frequencies in the theory of rigid bodies with a double porosity structure. In: Albers, B., Kuczma, M. (eds.) *Continuous Media with Microstructure 2*, pp. 287–306. Springer International Publishing, Switzerland (2016)
- Svanadze, M.: Steady vibration problems in the theory of elasticity for materials with double voids. *Acta Mech.* **229**(4), 1517–1536 (2018)
- Singh, D., Kumar, D., Tomar, S.K.: Plane harmonic waves in a thermoelastic solid with double porosity. *Math. Mech. Solids* **25**(4), 869–886 (2020)
- Biswas, S., Abo-Dahab, S.M.: Reflection of P-waves in porous thermelastic solid with three-phase-lag model. *Waves Random Complex Media* **32**(5), 2105–2123 (2022)
- Long, J., Fan, H.: Effects of interfacial elasticity on the reflection and refraction of SH waves. *Acta Mech.* **233**, 4179–4191 (2022)
- Kumar, A., Tomar, S.K.: Coupled dilatational waves at a plane interface between two dissimilar magneto-elastic half-spaces containing voids. *Acta Mech.* (2022). <https://doi.org/10.1007/s00707-022-03353-w>
- De Cicco, S.: Non-simple theory of elastic materials with double porosity structure. *Arch. Mech.* **74**(2–3), 127–142 (2022)
- Straughan, B.: *Mathematical Aspects of Multi-porosity Continua*. Springer, Cham (2017)
- Eringen, A.C., Edelen, D.G.B.: On nonlocal elasticity. *Int. J. Eng. Sci.* **10**, 233–248 (1972)
- Eringen, A.C.: Linear theory of nonlocal elasticity and dispersion of plane waves. *Int. J. Eng. Sci.* **10**, 425–435 (1972)
- Eringen, A.C.: *Nonlocal Continuum Field Theories*. Springer-Verlag, New York (2002)
- Altan, S.B.: Uniqueness in the linear theory of nonlocal elasticity. *Bull. Tech. Univ. Istanbul.* **37**, 373–385 (1984)
- Altan, S.B.: Uniqueness of initial-boundary value problems in nonlocal elasticity. *Int. J. Solid. Struct.* **25**(11), 1271–1278 (1989)
- Chirita, S.: On some boundary value problems in nonlocal elasticity. In: *Amale Stinifice ale Universitatii “AL. I. CUZA” din Iasi Tomul. 22* (1976)
- Shaat, M., Ghavanloo, E., Fazelzadeh, S.A.: Review on nonlocal continuum mechanics: physics, material applicability, and mathematics. *Mech. Mater.* **150**, 103587 (2020)
- Singh, D., Kaur, G., Tomar, S.K.: Waves in nonlocal elastic solid with voids. *J. Elast.* **128**(1), 85–114 (2017)
- Khurana, A., Tomar, S.K.: Reflection of plane longitudinal waves from the stress-free boundary of nonlocal, micropolar solid half-space. *J. Mech. Mater. Struct.* **8**(1), 95–107 (2013)
- Khurana, A., Tomar, S.K.: Wave propagation in nonlocal microstretch solid. *Appl. Math. Model.* **40**(11–12), 5858–5875 (2016)
- Khurana, A., Tomar, S.K.: Waves at interface of dissimilar nonlocal micropolar elastic half-spaces. *Mech. Adv. Mater. Struct.* **26**(10), 825–833 (2019)
- Kalkal, K.K., Sheoran, D., Deswal, S.: Reflection of plane waves in a nonlocal micropolar thermoelastic medium under the effect of rotation. *Acta Mech.* **231**, 2849–2866 (2020)
- Das, N., De, S., Sarkar, N.: Reflection of plane waves in generalized thermoelasticity of type III with nonlocal effect. *Math. Appl. Sci.* **43**(3), 1313–1336 (2020)
- Kumar, S., Tomar, S.K.: Reflection of coupled waves from the flat boundary surface of a nonlocal micropolar thermoelastic half-space containing voids. *J. Therm. Stress.* **44**(10), 1191–1220 (2021)

32. Kumar, D., Singh, D., Tomar, S.K., Hirose, S., Saitoh, T., Furukawa, A.: Waves in nonlocal elastic material with double porosity. *Arch. Appl. Mech.* **91**, 4797–4815 (2021)
33. Borchardt, R.D.: *Viscoelastic Waves in Layered Media*. Cambridge University Press, Cambridge (2009)
34. Eringen, A.C.: Theory of nonlocal elasticity and some applications. *Res. Mech.* **21**, 313–342 (1987)
35. Eringen, A.C.: Plane waves in a nonlocal micropolar elasticity. *Int. J. Eng. Sci.* **22**(8–10), 1113–1121 (1984)
36. Ainslie, M.A., Burns, P.W.: Energy conserving reflection and transmission coefficients for a solid-solid boundary. *J. Acoust. Soc. Am.* **98**(5), 2836–2840 (1995)
37. Singh, D., Tomar, S.K.: Longitudinal waves at a micropolar fluid/solid interface. *Int. J. Solids Struct.* **45**(1), 225–244 (2008)

Publisher's Note Springer Nature remains neutral with regard to jurisdictional claims in published maps and institutional affiliations.